A new simplified method to estimate global longitudinal strain in oncology patients

by

Naji Kholaif

A thesis submitted in partial fulfillment of the requirements for the degree of

Master of Science
in
Translational Medicine

Department of Medicine
University of Alberta

Abstract

Background:

Global longitudinal strain (GLS) is currently a widely applied method to evaluate early left ventricular dysfunction in the oncology population. Its ability to predict left ventricular dysfunction is valid even in patients with normal ejection fraction. A significant limitation is its dependency on image quality. Suboptimal acoustic windows and in plane displacement result in considerable inter- and intra-observer variability. To overcome this limitation we sought a simplified method to estimate global longitudinal strain using few user-defined tracking points of the left ventricle.

Methods:

In 106 consecutive oncology patients who underwent echocardiography to evaluate for possible cardiotoxic effects of cancer medications as per current guidelines, additional simple strain measurements were performed. Using a tool of the Philips Q-lab software called 'user defined measurements' areas in the mitral ring and apical pericardium are tracked that have prominent speckles and are less confounded by noise. The percentage shortening of the distance between the mitral ring and the apex was measured in each of the 4 walls of the 2- and 4-chamber views and the average was reported as global simple strain. These values were compared standard GLS measurements.

Results:

The mean age was 55.6 years. 84% of study population were females. The mean ejection fraction was 61.2 ± 8.5. Of the study population 80% had no wall motion abnormality. GLS values were higher than simple global strain values, -20.5 ± 2.6% and -12.3 ± 2.6%, $P < 0.05$. There was a strong linear correlation between GLS and simple global strain ($r= 0.7$) which was superior to the correlation of each method with ejection fraction ($r=0.54$ for GLS and $r=0.38$ for simple strain).

The inter-observer variability for the simplified method was tested in 22 patients and in 20 for GLS. The mean absolute difference in the simple global method was 0.25±0.22% and 1.1±1.0% for GLS. The mean relative standard error was 2.4% for the simplified method and 5.6% in GLS. Bland-Altman analysis showed a small bias (0.11) with a narrow limits of agreement (1.96 x SD), -0.5 to 0.73%. The beat to beat variability was tested in 12 patients, the mean absolute difference was 0.43±0.32% and the mean relative standard error was 3.7%. There was a small bias (-0.18) with narrow limits of agreement (1.96 x SD) -1.2 to 0.85%.

Conclusion:

The simplified strain method using tracking areas at the apex and base of the heart showed good correlation with the standard speckle-tracking GLS method. This method is less time consuming, the tracking is easier to evaluate and is less affected by image quality. It has good inter-observer and beat to beat variability. This method could potentially supplement and in some cases replace GLS - particularly in patients with poor acoustic windows.

Preface

This thesis is an original work by Naji Kholaif. The research project, of which this thesis is a part, received research ethics approval from the University of Health Research Ethics Board of Alberta Cancer Committee “A Registry for Cardiac Function in Patients Treated for Various Types of Cancer” , HREBA.CC-16-0309.

Table of Contents

List of Figures

are tracked during the entire cardiac cycle and the longitudinal strain is automatically calculated.

Fig.8 Processing steps to measure simplified strain: A. Select 4-chamber view. B. regions of interest are placed using a user defined program (see yellow arrows). The septal mitral annular ring and its corresponding epicardial apex location are chosen (in blue) then the lateral annular ring of the mitral valve with its corresponding epicardial apex are chosen (in orange). C. & D. the regions of interest are tracked and the percentage of shortening is automatically calculated. -starting from the beginning of systole for an entire cardiac cycle.

Fig.9 This curve is generated from continuous tracking throughout the cardiac cycle. The "X" axis shows time though the cardiac cycle in seconds, while the "Y" axis demonstrate shortening in percentage points (strain). It starts at the beginning of systole (aortic valve opening) as is shown by the first yellow arrow and it is the highest point in the curve while the second arrow shows the end of systole (aortic valve closure). The green box delineates systole. The third arrow shows diathesis which is often not completely horizontal. The fourth arrow directs to the change following atrial contraction.

Fig 10 measurement of GLS; strain curves of the 4-chamber view (upper left) 2-chamber view (upper right) and 3-chamber view (lower left) are shown as well as a bulleys view (lower right) For each view a GLS value is computed. In the echocardiography report the average of all segmental GLS measurements is inserted

Fig.11 simple strain measurement in the 4-chamber view. The blue curve represents the septal motion. Note the red dot on the strain curve which shows the maximum systolic strain, 12,5%. The red curve shows the strain of the lateral wall. The dotted line represents the average strain of the septal and lateral walls.

Fig.12 Kolmogorov-Smirnov test for normal distribution of the GLS measurements

Fig.13 Histogram showing distribution of the global simple strain measurements

Fig.14 Kolmogorov-Smirnov test for normal distribution of the simple strain values

Fig.15 Linear regression between the global simple method and GLS using the simple global method as an independent factor. The correlation coefficient was 0.87 (confidence interval: 0.7-1.0) P-value < 0.001. The unstandardized equation was $\bar{Y}=9.87+0.87(x)$

Fig.16 The relative mean errors in GLS for Philips echocardiography machines according to Farsalinos, Voigt et al.[48] , GLS in our study and global strain using the new simplified method. The "*" signifies statistical significance ($p < 0.05$).

Fig.17 Shortening of the myocardium assessed by GLS (yellow arrows) vs simple strain (green arrow)

List of Abbreviations

aCMQ	automated cardiac motion quantification
AVC	aortic valve closure
EF	ejection fraction
GLS	global longitudinal strain
LV	left ventricular
MAPSE	mitral annular plane systolic excursion
MVC	mitral valve closure
ROI	region of interest
SD	standard deviation

Chapter 1

LV strain – methodology, clinical applications and limitations

Left ventricular ejection fraction (EF) is the most frequently used parameter for evaluating global left ventricular function which is integral for management and prognosis in patients with cardiac disease.[1,2] The accurate assessment of EF is usually done by manually tracing the endocardial border in systole and diastole in transthoracic echocardiography. This is time consuming, and limited by poor image quality and possibly by foreshortened apical views.[3]

In recent years automated techniques have evolved for border detection but they depend on good acoustic windows. The administration of echocardiographic contrast agents enhances the delineation of endocardial borders and is often needed when there are poor acoustic windows.[4]

Deformation imaging

During ventricular systole there is simultaneous shortening of the myocardium in its longitudinal and circumferential plane and thickening in its radial plane. Direct assessment of this shortening and thickening can be achieved by deformation imaging using strain and its derivative strain rate.[5,6] Deformation imaging has been validated in experimental models and in clinical studies using magnetic resonance imaging-based tagging and sonomicrometry crystals.[7,8]

Sophisticated techniques allowed for deformation imaging in echocardiography. This was achieved by tissue Doppler, and now more recently by 2-dimensional and three-dimensional speckle tracking imaging.[9]

Speckle tracking

The ultrasound speckle patterns are generated by the interference of the ultrasound waves reflected from tissue structures such as myocardial fibers.[5, 9] Looking at a two-dimensional echocardiogram one can see a grainy pattern of the myocardial tissue with speckles inside the myocardium (Fig.1). In speckle tracking, the movement of these speckles is assessed.

The method relies on the velocity vector and not simply the velocity component along the image scan line as in the case of Doppler and therefore it is not angle dependent.[10]

The speckle is a radiofrequency ultrasonic backscatter pattern which is identified within a frame as pixels grouped together to form a unit called a “Kernel”. The kernels are fairly stable within an ultrasonic frame. On the next frame a wider search area is done around the initial kernel and the position with the highest similarity is considered a solution and identified as in-plane displacement using the best match search algorithm (Fig.1). This motion is tracked using a Sum-Absolute-Difference (SAD) algorithm generating a vector map of 2D velocities.[11,12,13]

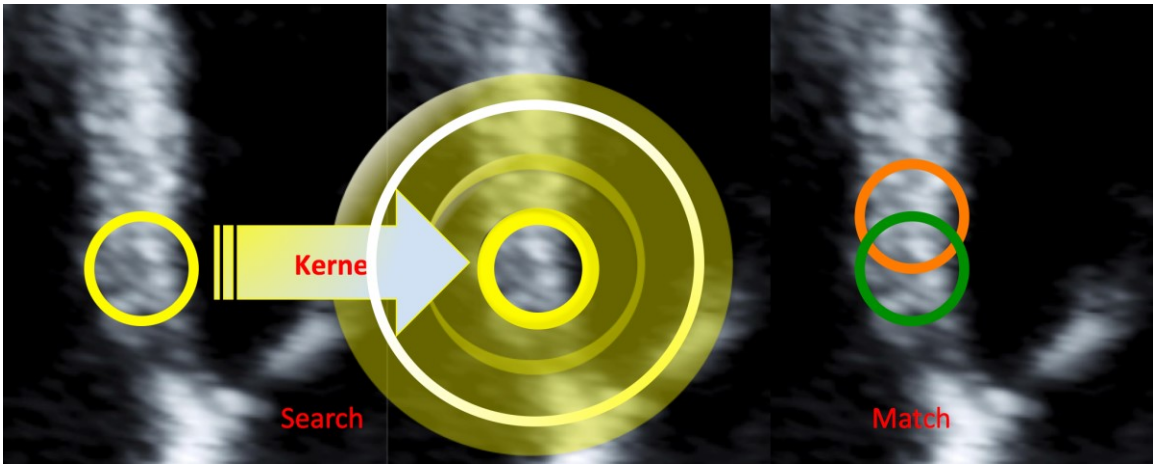

Fig.1 *Principle of speckle tracking. In the first image (A) a pattern of ultrasound scatter "speckles" is identified as a unit called "Kernel". This pattern is searched for in the subsequent frame (B) in a larger search area and then identified (C). The vector, displacement can then be tracked. By measuring the distance between adjacent kernels the strain is calculated.*

Strain measurement -principle

Strain in general describes the deformation of an object relative to its original state. Strain rate is the rate of deformation (how fast this deformation occurs).

To simplify, in a theoretically one dimensional object deformation can be either shortening or lengthening. To calculate this either Lagrangian or natural strain methods are used.

In Lagrangian strain, a certain reference length is defined (Lo). Subsequent deformation of lengths (L_1) is reported in relation to the refrence length . The Lagrangian strain rate is simply the derivative of Lagrangian strain (Fig.2).[9]

$$\text{Strain } (\varepsilon) = L_1 - Lo \,/\, Lo \quad .$$

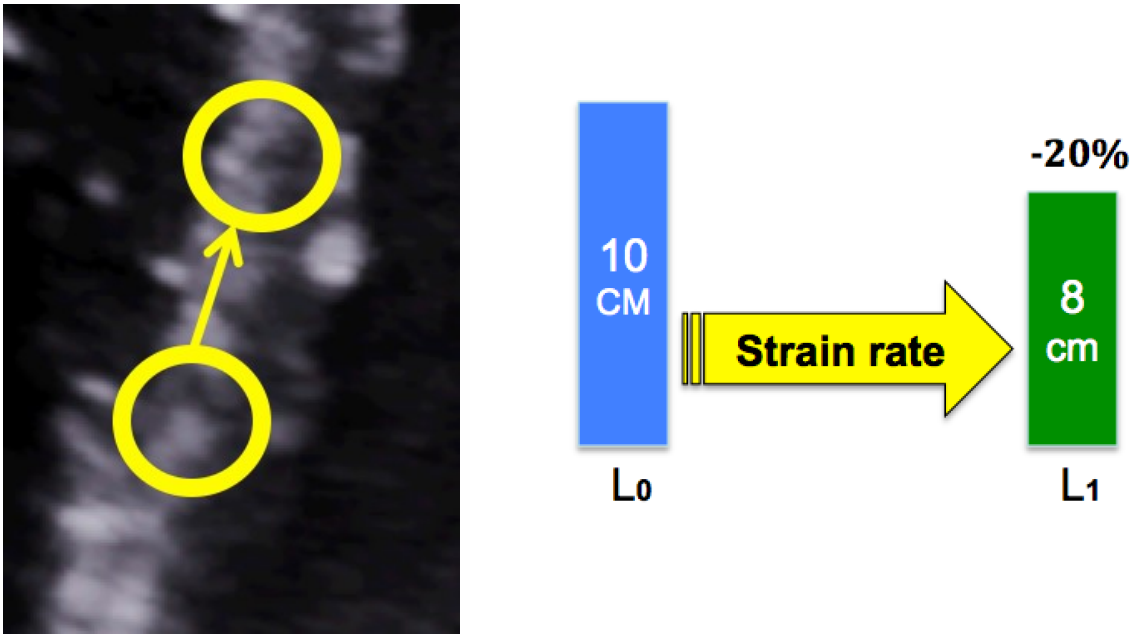

Strain (ε) = L_1 – Lo / Lo

Fig.2 *Principle of strain measurement. There are two areas of speckles shown on the left. The distance between the areas can be calculated by tracking the two areas. To simplify the concept of speckle tracking, the length in end-diastole is taken as the reference length L_0 (in longitudinal strain for example). During systole the two speckle areas move towards each other and the shortest distance is found in systole-diastole L_1. The strain rate is the rate by which the shortening occurs.*

In natural strain, the reference length changes with object deformation. It describes instantaneous changes. This method is usually used in Doppler but not needed in speckle tracking since the baseline length is known and can be used as reference.[14]

Types of Strain measurement including geometry of the myofibers:

The myocardial fibers differ from skeletal muscles in the sense that they lack a clear origin and insertion. The myo-architecture is a transmural continuum with two helically oriented groups of fibers.[15] While the orientation of the fibers is circumferential in the middle layer of the LV myocardium, the fibers are oriented in a longitudinal direction in the sub-endocardial layers.[16] Longitudinal strain measurements are applied to assess the shortening of the myocardial fibers in the sub-endocardial layers, while the other layers are assessed by circumferential and radial strain.

How to measure strain?

It is arbitrary to select a reference point in time to determine the beginning of a cardiac cycle since it is cyclical. However, end-diastole has been conventionally chosen to perform deformation measurements. End-diastole is usually defined as the last frame before the mitral valve completely closes (MVC). Surrogate markers are the peak of the R wave on ECG and the largest diameter of LV. The timing of end-diastole can be affected by wall motion abnormalities and conduction delays.[17] [18]

End-systole coincides with aortic valve closure (AVC) which can be detected by visualizing the aortic valve in the apical long axis or the closure click on a pulse-wave Doppler recording of the flow through the aortic valve. Alternatively the nadir of the global strain can be used.[9,19]

In order to initiate speckle tracking, the clinically available systems require to set regions of interest (ROI). It is important to track the speckles in the compact myocardium. Most analysis systems require only manual adjustment of the inner border of the ROI. In the Philips systems the tracking is initiated automatically after the operator has selected an appropriate loop and ticked the box to identify the loop as 4-, 2- or 3-chamber view.

The endocardial border is defined as the border between the compact and trabeculated myocardium. From the endocardial border the ROI extends 1 cm towards the epicardium, but this can be adjusted. The contours can be either manually traced or delineated by an automated contour finding algorithm with the ability to manually adjust the contour (Fig.3).

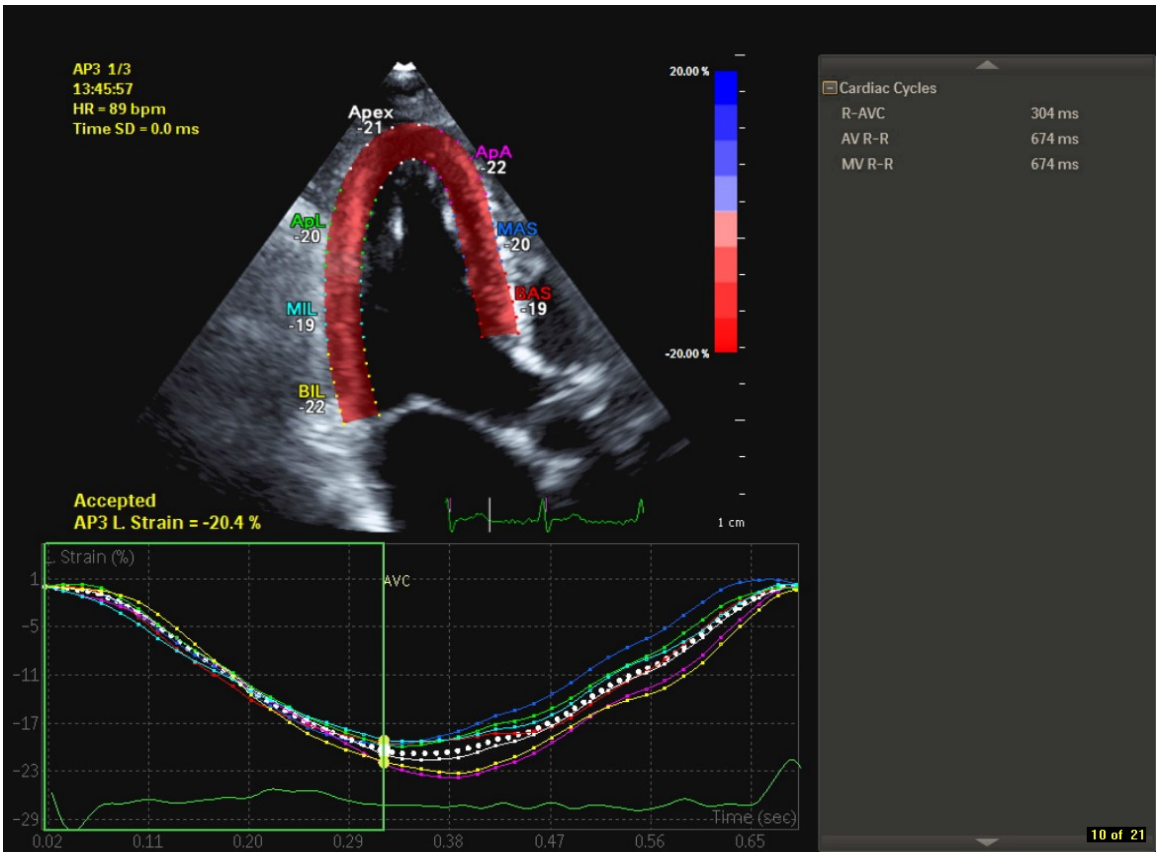

Fig.3 *Longitudinal strain curves obtained in the 6 segments of the 3-hamber view. On the y-axis the strain is plotted. The systole is highlighted by the green frame with the left side representing the aortic valve closure (AVC) which often coincides with the lowest point of the strain curves. The scale of the Y-axis ranges from 0 at end-diastole to -25%.*

All state-of-the-art systems for assessment of GLS provide measurements of segmental longitudinal strain and global longitudinal strain. The LV myocardium is divided into different segments similar to the segments used for assessment of regional LV function. In the apical views there are apical, mid-ventricular and basal segments. The segmentation of the myocardial segments is performed automatically after the tracking contour along the endocardium has been set. The endocardial tracking contour connects the hinge points of the mitral valve and the apex.[9] The GLS analysis tool used in this study includes 17 segments. In addition to 16 segments used for assessment of regional LV wall motion, a separate apical segment is included for assessment of longitudinal strain (Fig 4).[20]

Usually there are multiple speckles in a segment. Multiple pairs of Kernals are followed through the cardiac cycle, and the average of the strain measurements is reported as the segmental strain value. This is a vectorial quantity with a direction and amplitude. The vectors in the apical views are expressed in two ways:

The longitudinal component V_L is oriented tangential to the endocardial contour. Longitudinal strain values are usually negative. The distance between adjacent kernels is always related to the distance between the kernels in end-diastole. Shortening is reported as a negative value. The average of the longitudinal components in each segment are processed to obtain global longitudinal strain measurements.

The radial component V_r is oriented perpendicular to the endocardial contour. Here a positive value represents thickening of the myocardium as the distance of adjacent kernels increases in systole.

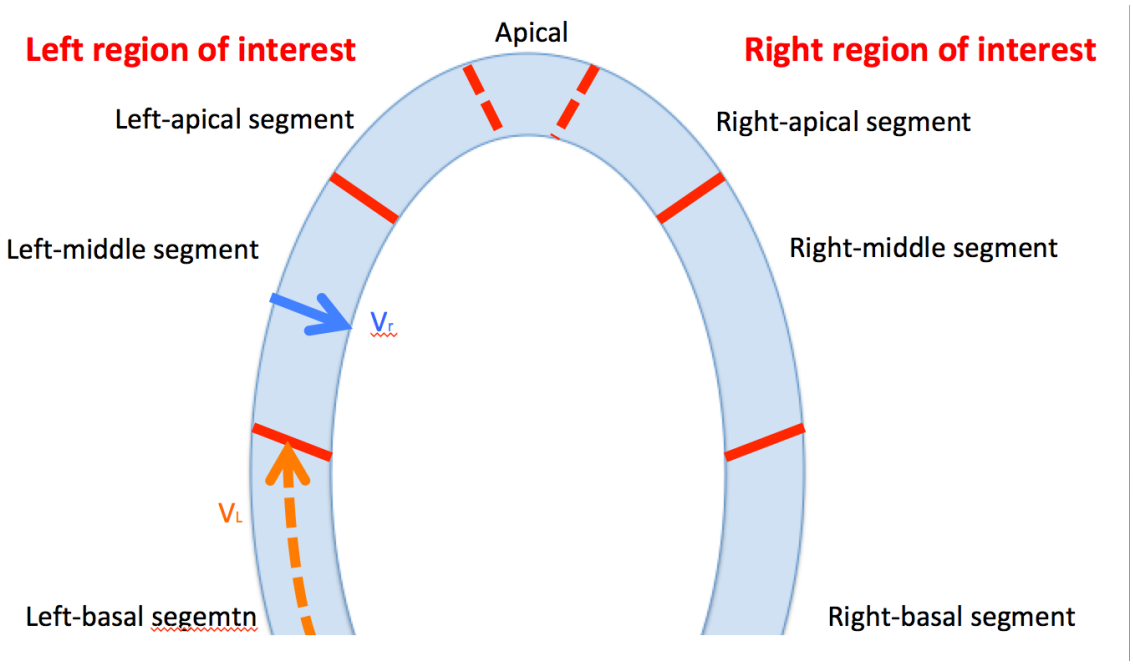

Fig 4 *In apical views the myocardium is divided into 6 (solid) or 7 (dashed lines) segments. The longitudinal strain component (V_L) is oriented tangential to the endocardial contour. A negative value represents shortening of the segment in relation to the end-diastolic length. The radial velocity vector (V_r) is perpendicular to the endocardial contour and it is positive when the myocardium thickens during systole.*

Strain measurements can also be performed in parasternal short-axis views similar to the measurements in apical views (Fig.5). The RV insertion is used to anatomically orient the ROIs. The short axis views are usually divided into 4-or 6-segments depending on the level of the short axis (Fig 5).

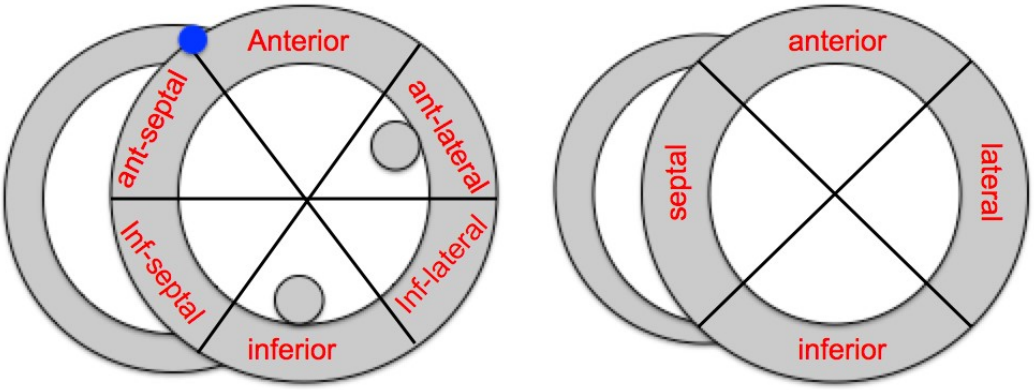

Fig.5 *Short axis view at the base of the heart (6 segments) and apex (4 segments). The blue dot is the anterior RV insertion point for orientation.*

In the short-axis views the displacement vectors have two components: V_r –the radial component that is perpendicular to the endocardial border and is positive when the myocardium thickens in systole. V_c –the circumferential component represents the change in the circumference in a segment, it is reported as degree per second change and is relative to the center of the cavity (Fig 6).

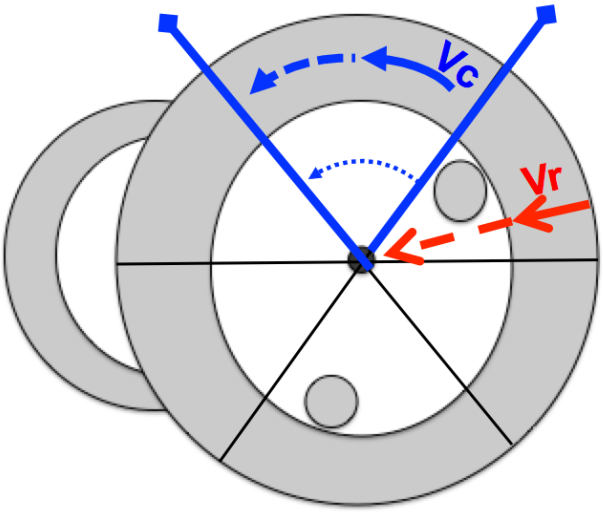

Fig.6 *Mid short axis view. The radial component of displacement (V_r) is perpendicular to the endocardial contour and it is positive in systole when the distance between adjacent kernels increases. The circumferential vector (Vc) is tangential with the endocardium*.

Types of strain measurement:

Longitudinal strain represents deformation along the long axis where the base moves towards the apex. It is measured in the apical views. Myocardial fibers shorten during systole reflected in individual kernels distance reduction giving an overall negative value. (Figure 4) Averaging the measurements in the 2-chamber, 3-chamber and 4-chamber views gives the global longitudinal strain, which is the most reproducible strain method, it is therefore the most used in clinical practice.[5]

Radial strain is deformation directed towards the center of the LV. It is measured in both apical and short axis views. It represents the thickening motion of the myocardium and is therefore positive in systole. (Figure 6)

Circumferential strain represents shortening of the myocardial fibers along the circumference of the LV. It is measured along the short axis views and has a negative value during systole. (Figure 6)

Twisting and untwisting can be assessed using short axis views: The apex rotates in a clockwise direction during systole and the base moves in a counterclockwise direction. Twisting is assessed by the measurement of the reciprocal rotation of the apex relative to the base of the heart in systole. The opposite occurs in diastole and is termed untwisting.[21 22]

Longitudinal strain vs mitral ring displacement

Before speckle tracking imaging became available, estimates of the longitudinal LV function could be obtained by assessment of the displacement of the mitral ring during systole using M mode. MAPSE (mitral annular plane systolic excursion) is a reflection of the hearts longitudinal function and is the major contributor to the overall LV systolic function.[3,23] It is represented by the movement of the mitral plain from the base of the heart towards the apex and it is equivalent to longitudinal shortening[23]. Mitral valve displacement has been observed to be reduced in a number of pathological conditions like cardiomyopathies, hypertrophic heart disease and valvular heart disorders. MAPSE also can be measured by speckle tracking imaging. There is a good correlation between measuring mitral valve displacement by M-mode and 2D longitudinal speckle tracking.[23,24] Unlike the measurements using M mode measuring mitral valve displacement by speckle tracking is angle independent.[24]

Measurement of mitral annular displacement is easy to perform and is less dependent on the image quality than the myocardial strain measurements, but MAPSE is currently not widely applied in clinical echocardiography. The displacement of the mitral ring is measured in cm. However, the amount of mitral ring displacement depends on the size of the left ventricle. This limitation can be overcome using the ratio of the mitral ring displacement to the end-diastolic LV length which has to be measured separately. This requires good image quality to obtain reliable measurements. The simple strain method takes advantage of the robust tracking of the mitral ring but also provides reliable assessment of the end-diastolic distance between the mitral ring and the apex.

Clinical use of speckle tracking:

Coronary artery disease:

In principle segmental strain measurements offer an objective assessment of regional LV function which appears to be very attractive considering the variability of the current visual semi-quantitative assessment. However, the variability of strain measurements is currently limiting the use of segmental strain in clinical practice (see next chapter). The use of strain has given insight to the mechanics of ischemia not only in the form of reduced peak strain, but also the concept of post systolic shortening.[25] This is the difference in timing between aortic valve closure and peak strain curve. The reason for this is that ischemic segments do not show early diastolic thinning and lengthening after AVC closure but ongoing post-systolic thickening and shortening.[26,27]

Cardiomyopathies:

In patients with cardiomyopathies, strain offers great promise in both early diagnosis as well as prognostic information compared to LV ejection fraction. IT also appears to be a more accurate marker of myocardial dysfunction than ejection fraction.[28] This is particularly evident in hearts with thick myocardium, where ejection fraction can be normal but because the LV has a smaller cavity and changes in volume are under-estimated. Longitudinal strain is reduced in conditions like hypertrophic cardiomyopathy particularly in the inter-ventricular septum. It has been incorporated in recent guidelines.[29] The insights of the mechanical dysfunction that can be detected in deformation studies, can help differentiate otherwise morphologically similar cardiomyopathies.[30] One particularly specific example is cardiac amyloidosis which shows often preserved longitudinal strain of the apical segments but significant reduction in the mid and basal segments.[31] Reduced longitudinal strain in the posterior and lateral segments might suggest Fabry disease corresponding to hypertrophied papillary muscle.[32] However the pattern of reduced strain becomes more diffuse as cardiomyopathies progress.

Valvular heart disease:

In patients with moderate to severe lesions who are asymptomatic, the timing of surgery remains a challenge. Reduction in LV ejection fraction is usually a late consequence and might represent irreversible myocardial damage. Strain has been shown to have added clinical value in severe aortic and mitral regurgitation as well as in aortic stenosis.[33] [34] Larger prospective studies are needed to see if earlier surgery can be guided by changes in strain.

Cardiotoxicity:

Several studies have shown strain to be a sensitive a reliable tool in detecting subclinical LV dysfunction in cancer patients undergoing chemotherapy.[35] When cardiotoxicity was defined as a reduction of LVEF of > 10% to an EF < 55% GLS has been shown to be a better predictor of worsening cardiac function during chemotherapy than pro-BNP level and LVEF. GLS was also shown to have a better

intra-observer and inter-observer variability compared to LVEF.[36] Clinical heart failure was not seen in patients who had GLS > -19%.[37] In addition, initiation of cardioprotective medications has the potential to ameliorate a lot of the cardiac complications seen in these patients.[38] For this reason, GLS has been included in the recommendations for monitoring cancer patients receiving cardiotoxic drugs and should be available in all specialized cardio-oncology clinics in order to guide management with potentially early initiation of therapies before reduction in LVEF.

Cardiac resynchronization therapy:

In normal myocardium there is minimal difference in the timing of the peak systolic strain between the myocardial segments. However, there can be major differences in the time from end-diastole to peak systole in patients with left bundle branch block or other conditions which lead to intraventricular dyssynchrony. Cardiac resynchronization therapy has been shown to improve cardiac function and outcomes in a group of patients with low ejection fraction and wide QRS.[39] There are reports of an incremental value of strain measurements to predict CRT responders.[40] In the group of patients who respond to resynchronization therapy, a novel index of diastolic strain rate to early mitral inflow (E/SR_{IVR}) have been able to predict diastolic improvements and was more accurate then E/E' ratio in predicting filling pressures. Similar results were reported after ST-elevation myocardial infarction.[41,42]

Limitations of strain measurements

Several factors can affect speckle tracking resulting in inaccurate strain measurements:

Tracking quality may be suboptimal if regions of the myocardium are poorly visualized. Stationary image artefacts (reverberations) can compromise speckle recognition. This also can happen when spatial or temporal resolution of the image acquisition is insufficient. [9,43,44] Speckle decorrelation can arise from out-of-plane motion, non-uniform motion of the sub-resolution scatters and non-uniformity of the ultrasound field.

The speckle tracking algorithm is dependent on the stability of the speckle pattern and is affected in areas where decorrelation is high, yielding inaccurate motion estimates. The LV base and apex are the most stable and least affected by noise.[3]

Because strain measurements are dependent on image quality, inter-observer variability is a problem. The feasibility was 88% and the coefficient of variation was 3.5% for the inter-observer variability.[45] In a study by Huqi and Becher, patients with good quality images showed closer agreement (inter-observer variability mean bias -0.39 $\pm$ 2.1, 95% limit of agreement -4.5 - 3.76) and good correlation with GLS measured by MRI ($r = 0.89$, $P < 0.01$). However, in poor quality images, the agreement was worse (mean bias -1.99 SD?, 95% limit of agreement -11.3 - 7.28). The reproducibility was improved by using echo enhancing agents.[46] In clinical

practice the variability is probably worse and many echo labs do not perform strain measurements yet although most scanners are equipped with the appropriate tools.

Another limitation is inter-vendor and inter-software variability. It was therefore recommended to use the same vendor's equipment and the same software when doing serial measurement for a patient.[47] There are efforts to develop a common standard for speckle tracking but at present it is recommended that follow up with strain measurements should be performed with the same ultrasound scanner.

Need for development of a more reliable strain method

Considering the limitations of current strain methodology, there is a clinical need for a more robust approach to measure longitudinal LV function.

Chapter 2

Comparison of a new simplified method with the clinically used method to estimate global longitudinal strain

Study population

106 consecutive patients referred for echocardiography before or during chemotherapy with cardio-toxic drugs were included. The echocardiograms were performed at the University of Alberta Hospital in Edmonton. In all patients the global longitudinal strain (GLS) and left ventricular (LV) ejection fraction (EF) were measured according to the ASE guidelines as long as the image quality was adequate for strain imaging. Additional simple strain measurements were performed using a tool of the Q-lab software called user defined measurements. The study was approved by the local IRB and informed consent was obtained for processing anonymized recordings.

Methods

The echocardiograms were performed using an Epiq7 (Philips) echocardiographic scanner and the GLS strain assessed in the 4, 3, and 2 chamber views using Q lab (version: 10.2) and Xcelera (version: R3.3L1 SP2 3.3.1.1103) software by Philips Medical Systems.

The GLS measurements were performed on the echocardiography scanner by the sonographer after all echo recordings had been stored. The sonographer also measured the LV ejection fraction with contrast agent using the Simpson biplane method of discs.[47]

Table 1 Principles of simple longitudinal strain measurement

1. Few tracking points
2. Tracking fibrotic tissue rather than myocardium
3. Only 2 apical views

Simple strain method

Because of the limitations in global longitudinal strain a simplified method was developed. The three principles of the proposed simple stain method are listed in table 1. The method relies on few tracking points in areas with prominent speckles which are less confounded by noise. In order to perform measurements of longitudinal shortening (strain) we were looking for an easy to track region in the apex and at the base of the heart. In the apical views the fibrotic annulus of the mitral valve usually provides strong speckles. In the apex, the endocardial border of the myocardium is often not well displayed but there is usually a stronger and more consistent signal from the pericardial/epicardial interface.

In the 4-chamber view, we chose areas of interest on the mitral ring, one at the base of the lateral wall and the other at the base of the septal wall (Fig.7, 8). Then we chose a corresponding region of interest on the epicardial surface of the apex. We decided to choose the epicardium rather the endocardial interface of the apex, because it has more prominent speckles since it is a fibrous structure and is therefore more stable. In consecutive frames, the program is able to track the speckle signature (area of interest) throughout the cardiac cycle. The regions of interest (ROI) for speckle tracking are set manually at end-diastole and then the tracking algorithm is initiated by pressing >compute<.

The result of the tracking algorithm can be seen on the screen with the ROI moving during display of the cardiac cycle. This allows us to visually control whether the ROI moves with the underlying heart structure. Only those recordings with good tracking were considered for further analysis. The ROIs at the mitral ring and the apex are connected by a line and one can see the shortening and lengthening of this line throughout the cardiac cycle.

Tracking at progressive time point throughout the cardiac cycle generates a curve representing the different strain values throughout the cardiac cycle (Fig.9). It starts with the aortic valve opening and progresses to aortic valve closure, which is usually the lowest point in the curve. The “X” axis represents the time. The recording starts at the beginning of systole. On the “Y” axis the strain values are plotted with a Zero value at the beginning. The percentage shortening (strain) is represented by a negative number. From the strain curve the strain rate curve can be computed. This is also provided by the software.

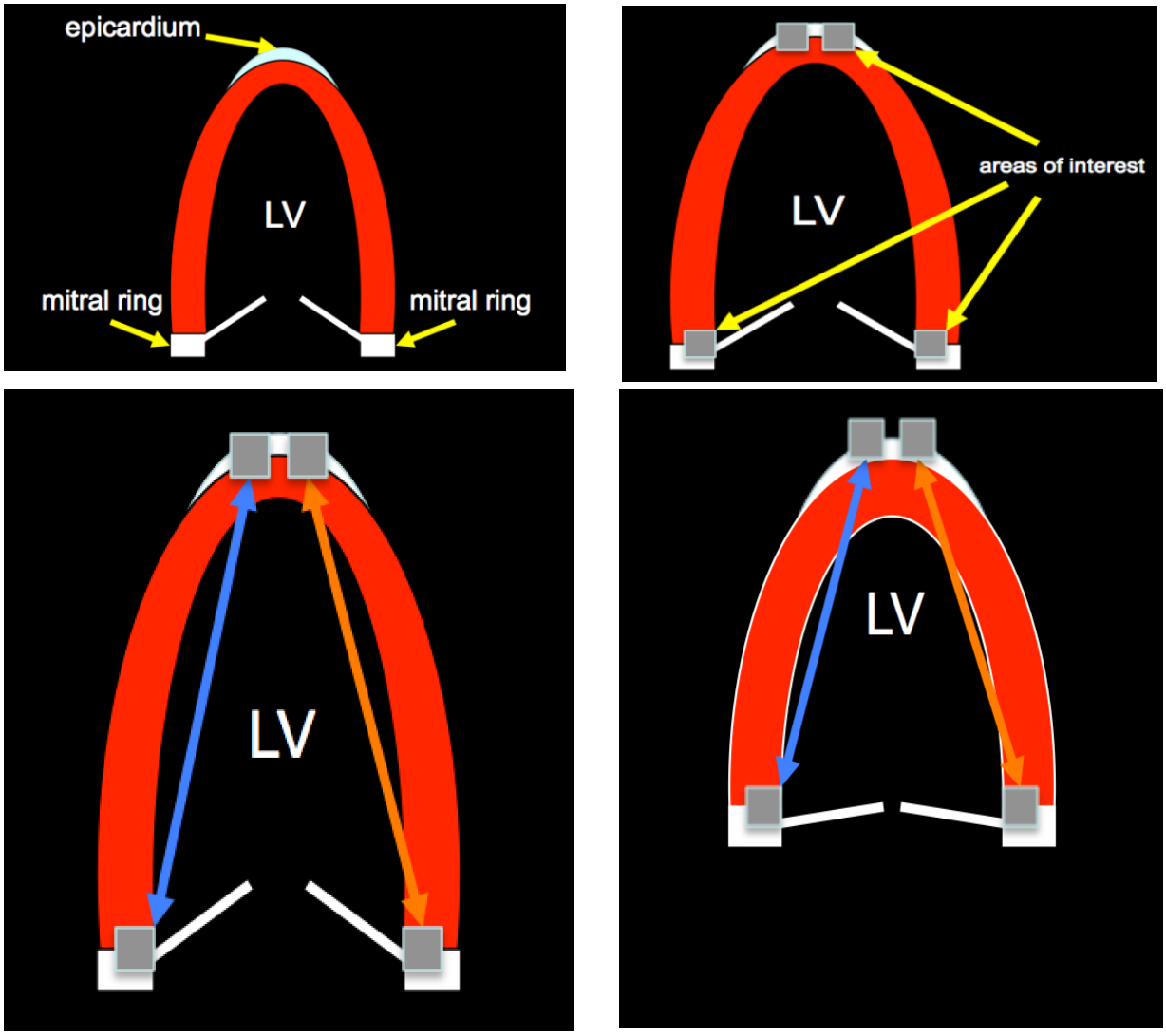

Fig.7 *Illustration of the simplified strain method. Top left: the yellow arrows point towards the mitral ring and the epicardium/pericardium which are the areas with the strongest speckle signal. Top right: regions of interest are chosen using a user defined program. Botto:. regions of interest tracked from the mitral ring towards the apex in diastole to systole. The change of the distance between mitral ring and apex over time is shown Fig.9.*

Step 1: Activate **aCMQ** (arrow)

Step 2: Select **User Defined**

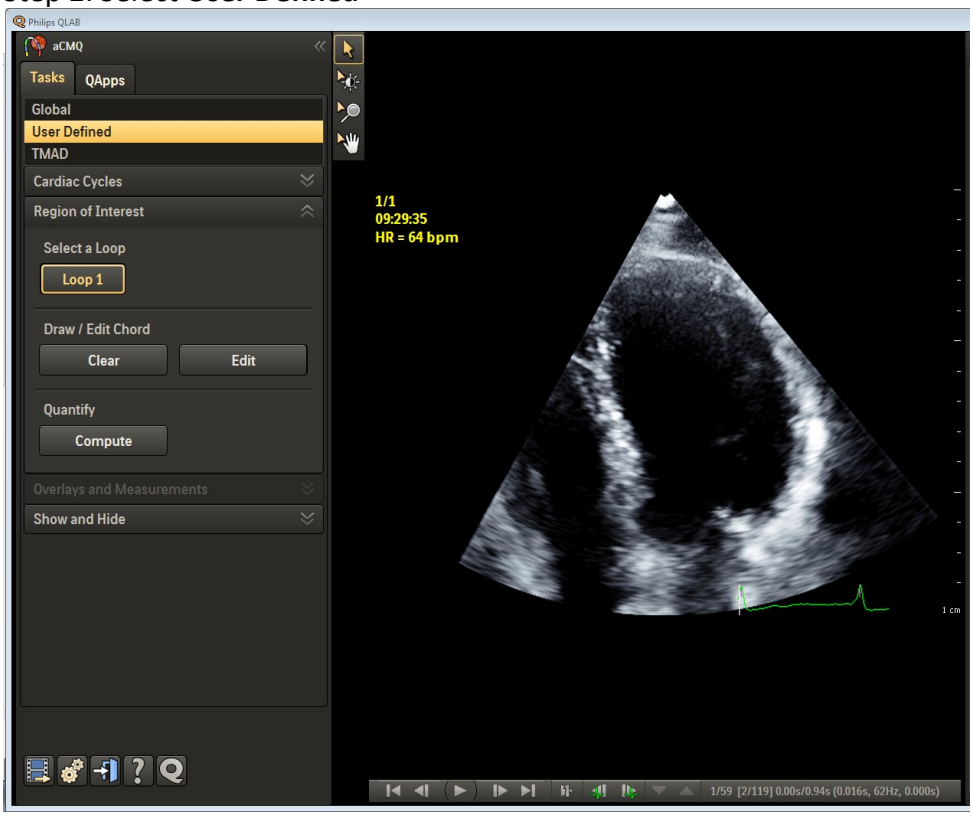

Step 3: Use the **cursor** and click on the septal mitral annulus and then on the apical peri-/epicardium.

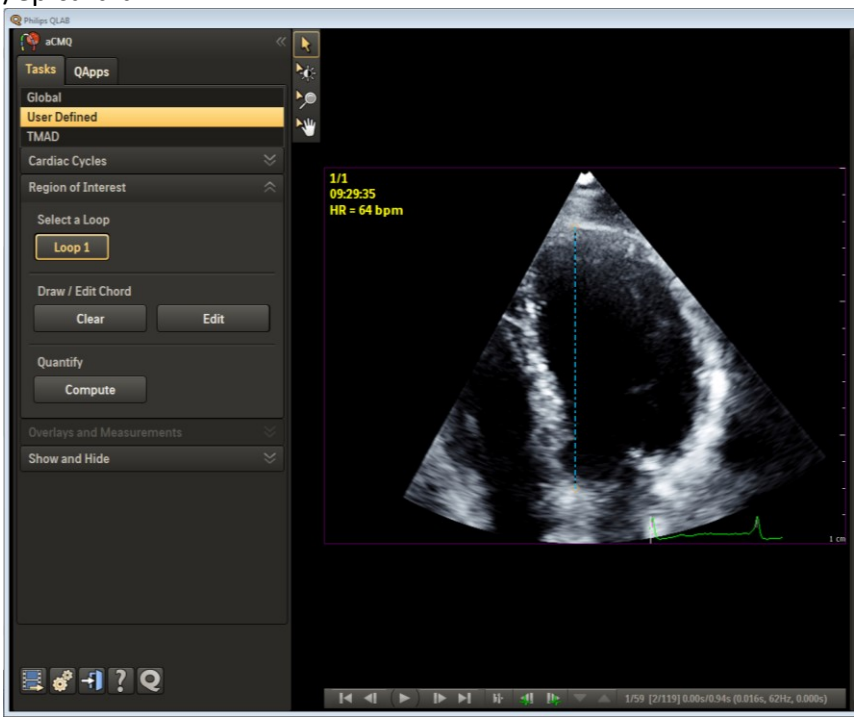

Step 4: Use the **cursor** and click on the lateral mitral annulus and then on the apical peri-/epicardium

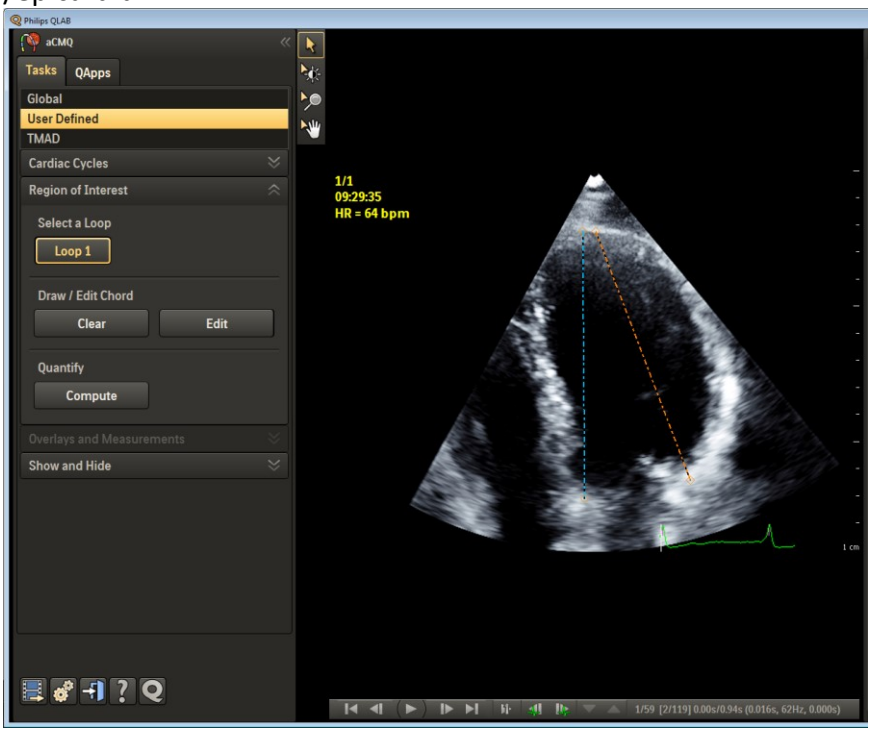

Fig.8 *Processing steps to measure simplified strain. Step1: Select 4-chamber view. Step 2: Select <user defined>. Step3: Using a cursor regions of interest are placed at the septal mitral ring and the apical epi-/pericardium (blue) then at lateral annular ring and the apex (orange, step4). After pressing <compute> the regions of interest are tracked during the entire cardiac cycle and the longitudinal strain is automatically calculated.*

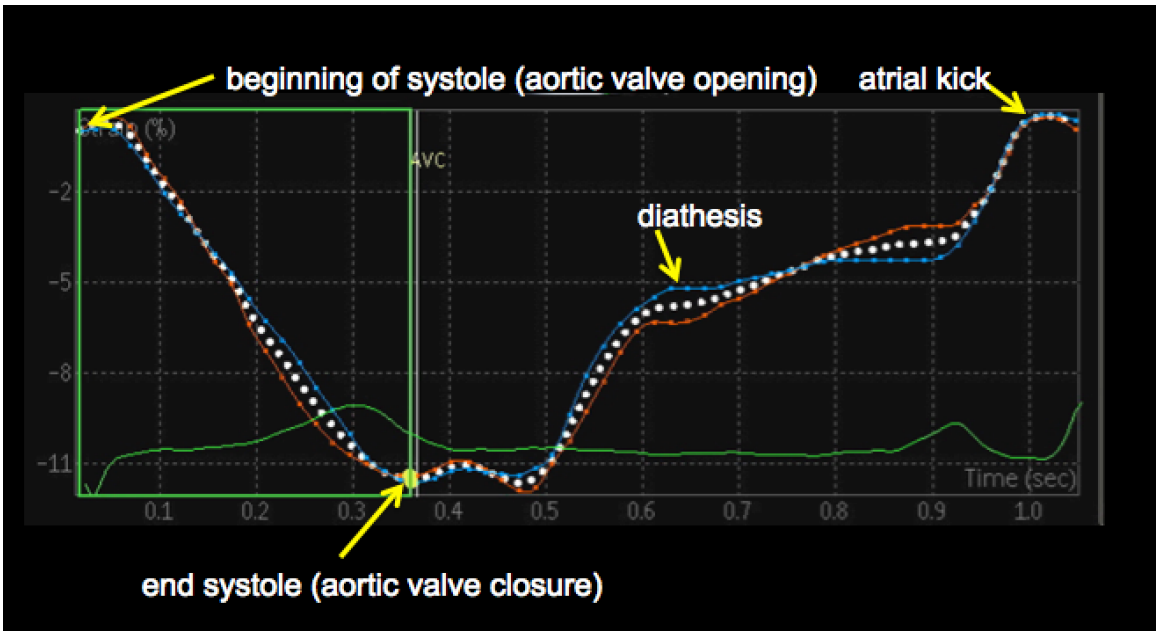

Fig. 9 *Simplified strain curve is generated from continuous tracking throughout the cardiac cycle. The "X" axis shows time though the cardiac cycle in seconds, while the "Y" axis demonstrates shortening in percentage points (strain). It starts at the beginning of systole (aortic valve opening) as is shown by the first yellow arrow and it is the highest point in the curve while the second arrow shows the end of systole (aortic valve closure). The green box delineates systole. The third arrow shows diathesis which is often not completely horizontal. The fourth arrow directs to the change following atrial contraction.*

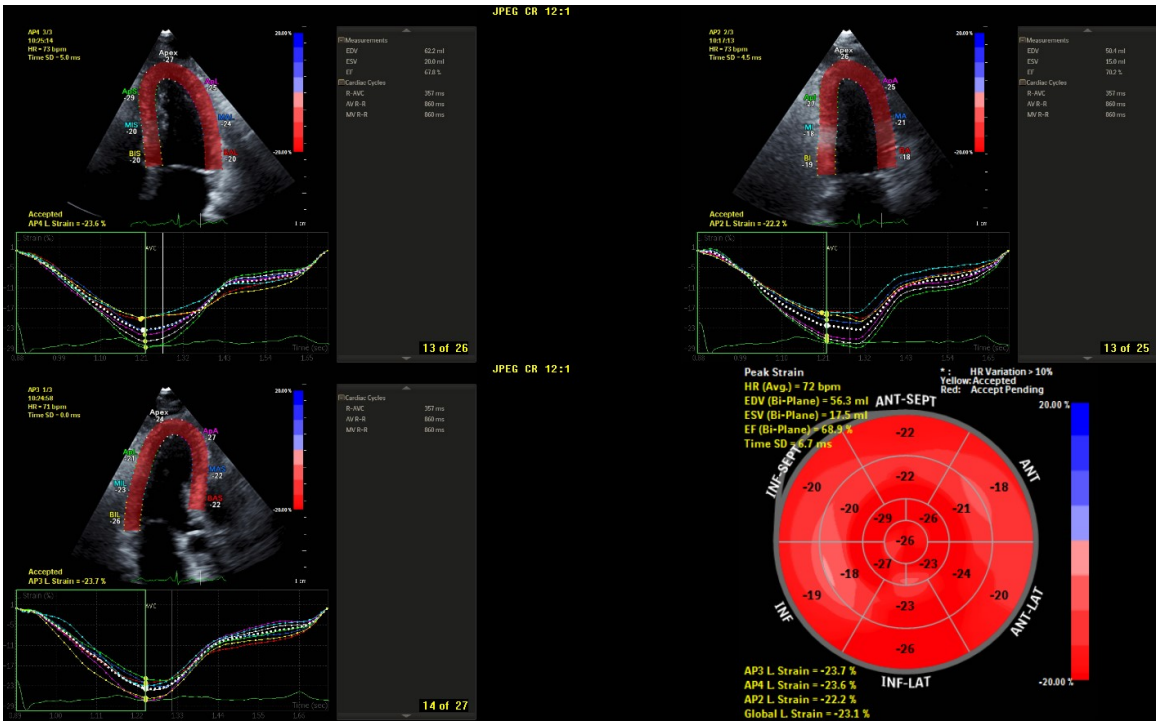

Fig. 10 *Measurement of GLS. Strain curves of the 4-chamber view (upper left), 2-chamber view (upper right) and 3-chamber view (lower left), as well as a bullseye view (lower right) are shown. For each view a GLS value is computed. In the echocardiography report the average of all segmental GLS measurements is inserted*

Global longitudinal strain measurement

The method has been described in detail in chapter 1. Using Qlab program Version 10.2 the 3 apical views were uploaded and GLS was measured (Fig.10).

Statistics

The distribution normality was assessed using a Kolmogorov-Smirnov test. The continuous values were expressed as mean ± SD. Pearson correlation was assessed between the GLS, simplified global strain as well LV ejection fraction. All statistics were two tailed and P values of < 0.05 was considered significant. Commercially available software was used (SPSS version 18; SPSS, Inc, Chicago, IL)

The mean and standard deviation of the peak systolic GLS was calculated by averaging the strain measurements from 2-chamber, 4-chamber and 3-chamber apical views. The mean and standard deviation of the Global Simplified Strain was calculated by averaging the simplified method measurements from 2-chamber and 4-chamber views. The simplified method was applied in 3-chamber view in only 20 patients to explore the applicability, but the results were not included in the analysis. In the following text unless indicated, we refer to absolute measurement values (i.e. GLS value of –20% will be expressed as higher than a GLS value of –16%).

To explore the normal values for the new simplified method, we divided the study population based on the GLS value. Since there were no recommended normal values for GLS, we decided to use a cutoff of -18% consistent with the lower normal value obtained by Philips systems in a recent inter-vendor variability study. [48]. Means and standard deviation was again calculated.

The inter-observer variability of the simplified method was evaluated by randomly choosing 22 patients from the overall cohort. Within 24 hours after the first measurement the simplified method was applied by an expert investigator who was blinded to the results of the other investigator. The beat to beat variability was evaluated in 13 patients, where the global simplified, and the GLS methods were used in two different beats. The mean and standard deviation was calculated for every wall. In addition, average values for the 2-chamber and 4-chamber views were reported as well as the average of all four wall measurements. GLS reproducibility was assessed in each of the three apical views. The relative standard error was then calculated by the ratio of absolute difference between the two measurements and the average of these two measurements.

Bland-Altman analysis was plotted to visualize the degree of agreement between the two readings and detect if there was fixed bias. The 95% limit of agreement (± 1.96 standard deviation of the difference) was plotted.

Results:

In all 106 patients simple strain measurements could be performed. Fig.11 shows an example of simple strain measurement in a 4-chamber view. For both strain methods the distribution of the measurements was found not deviating from the normal distribution (Fig. 12, 13, 14). A histogram of the GLS was found to be symmetrical.

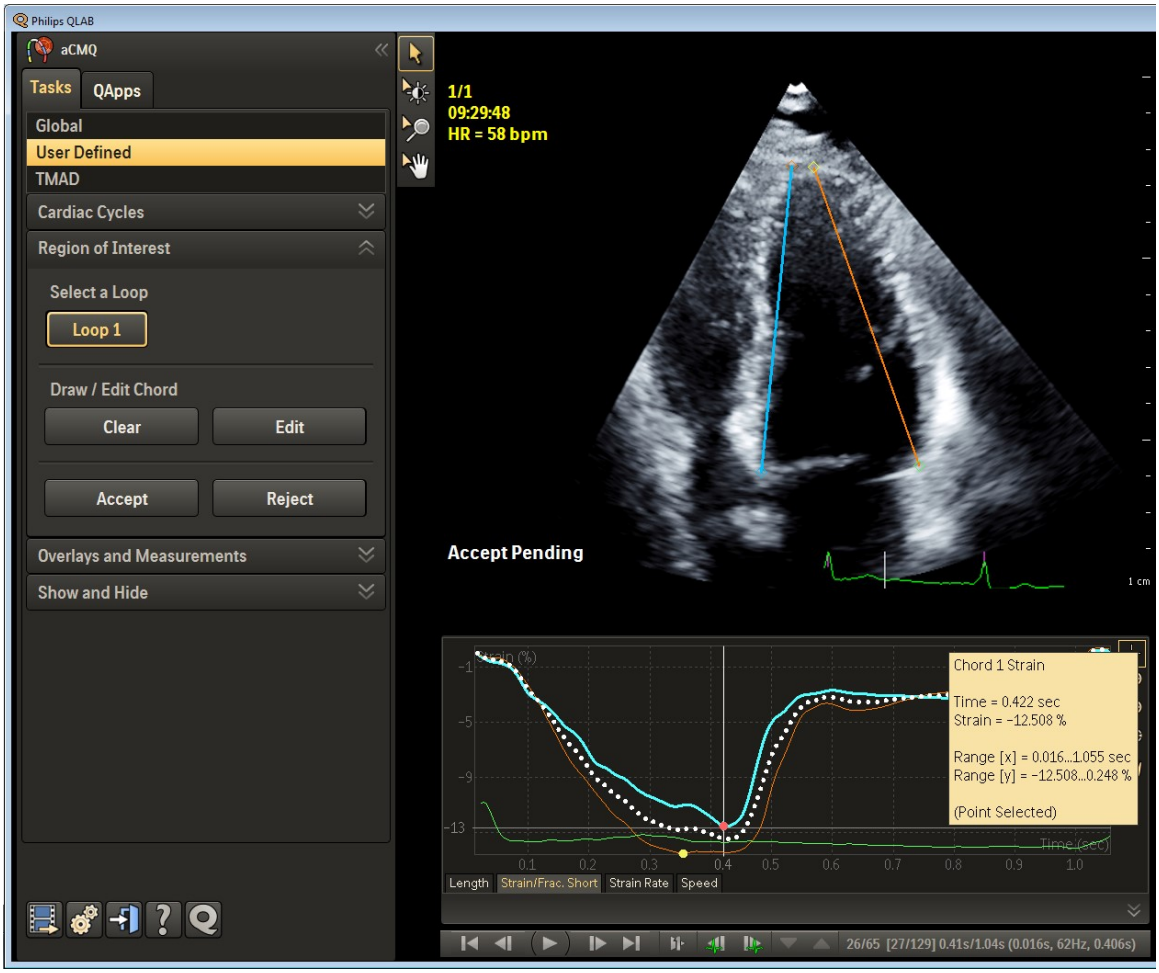

Fig.11 *Simple strain measurement in the 4-chamber view. The blue curve represents the septal motion. Note the red dot on the strain curve which shows the maximum systolic strain, -12,5%. The red curve shows the strain of the lateral wall. The dotted line represents the average strain of the septal and lateral walls.*

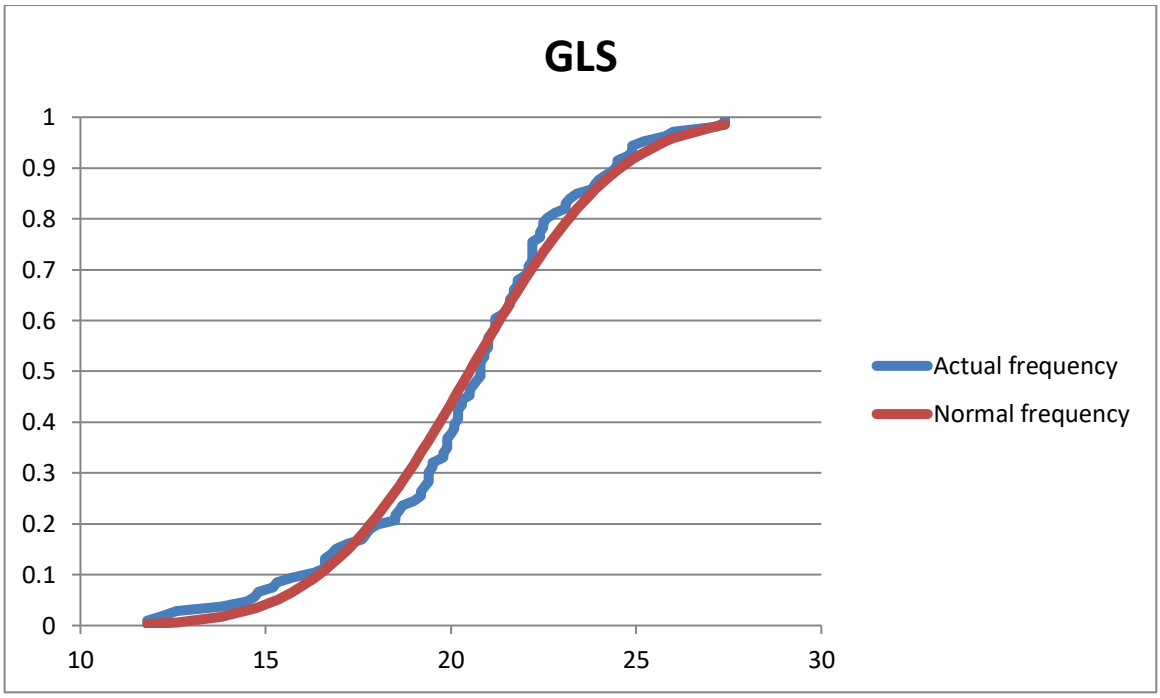

Fig.12 *Kolmogorov-Smirnov test for normal distribution of the GLS measurements*

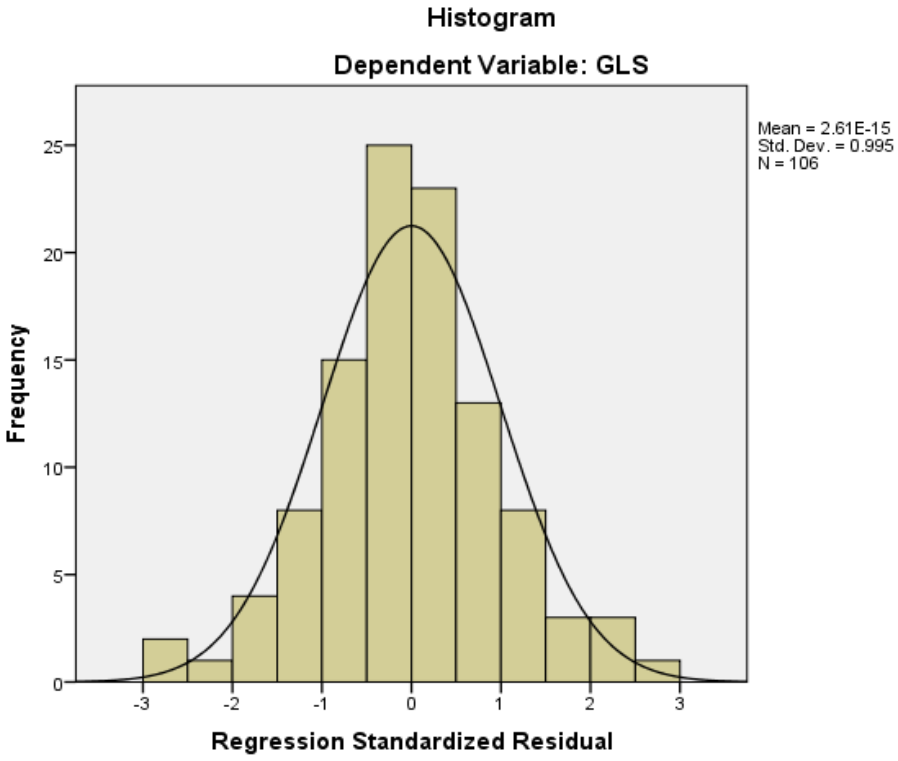

Fig.13 *Histogram showing distribution of the global simple strain measurements*

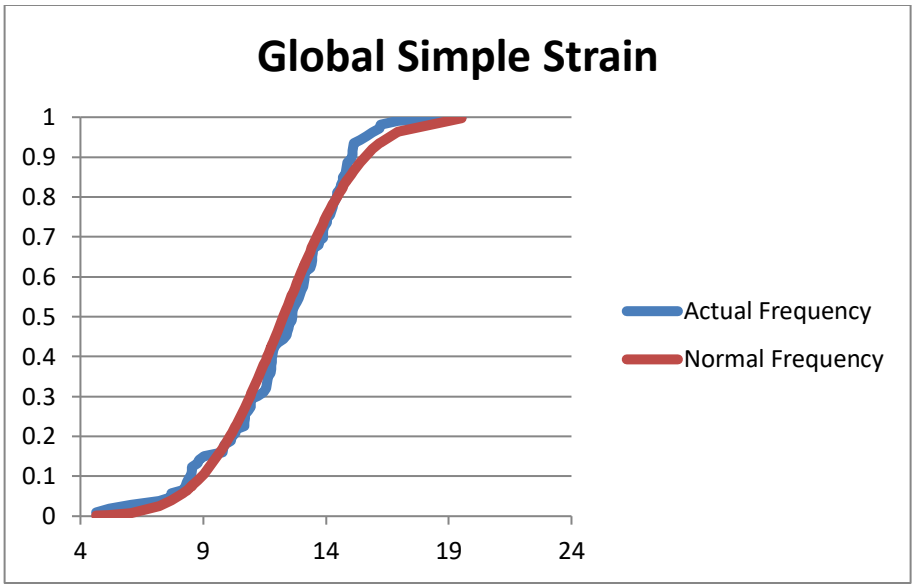

Fig.14 *Kolmogorov-Smirnov test for normal distribution of the simple strain values*

The mean age of the patients was 56 ± 13 years. 84% of the study population were females. The mean ejection fraction was 61.2 ± 8.5%. Of the study population 80% had no wall motion abnormality. The mean global longitudinal strain was -20.5 ± 2.6%. The mean value measured by the simple global method (average of 2 chamber and 4 chamber) was -12.3 ± 2.6%. The difference was statistically significant (p value < 0.000001). The simple strain measurements in the different LV walls and views are shown in table 2.

Table2 *Characteristics of the study population and simple strain measurements in different walls and views*

Mean age [years]	55.6 ± 13
Female patients	84%
Mean GLS	20.5% ± 2.6
Mean EF	61.2% ± 8.5
Simple strain - lateral wall	11.4% ± 3.1
Simple strain - septal wall	12.5% ± 2.7
Simple strain - anterior wall	12% ± 2.7
Simple strain - inferior wall	13.2% ± 3.3
Simple strain - 4-chamber view	12% ± 2.7
Simple strain - 2-chamber view	12.6% ± 2.8
Simple strain global (4-cv and 2-cv)	12.3% ± 2.6
Simple strain global (2-cv+4-cv+3cv)	11.34 ± 2.17

In a group of 22 patients, the simple global strain value was recalculated using all three apical views and was compared to corresponding values obtained from averaging the measurements of the 2-chamber and 4-chamber view. There was no statistical difference between the two groups (P = 0.11).

In order to explore the normal range of simple strain measurements, the mean and standard deviation was calculated in those patients who had GLS >18% and it was 13.1 ± 1.9%. In patients with a GLS < 18% the mean simple strain was 8.8 ± 2.2. The difference was statistically significant (P < 0.05).

Table 3 shows the correlations between the global simplified method (averaging the measurements in the 2-chamber and 4-chamber views), GLS and ejection fraction. The strongest correlation was between GLS and the global simple strain (r=0.7). This was better than the correlation between GLS and ejection fraction (r=0.54) and between the simple method and ejection fraction (r=0.38) (Tab.3).

Table 3 *Pearson correlation comparing Simple strain vs GLS vs LVEF.*

	r	**P-value**
Simple Global Strain vs. GLS	0.70361	<0.001
LVEF vs. GLS	0.54288	<0.001
Simple Global Strain vs. LVEF	0.37534	<0.001

The linear regression between global simple strain GLS is shown on Fig.15. The beta was 0.87 (confidence interval: 0.7-1.0, p-value < 0.001) (Fig.15). The correlation got worse, when the values in the 2-chamber view or the 4-chamber view were compared (see appendix).

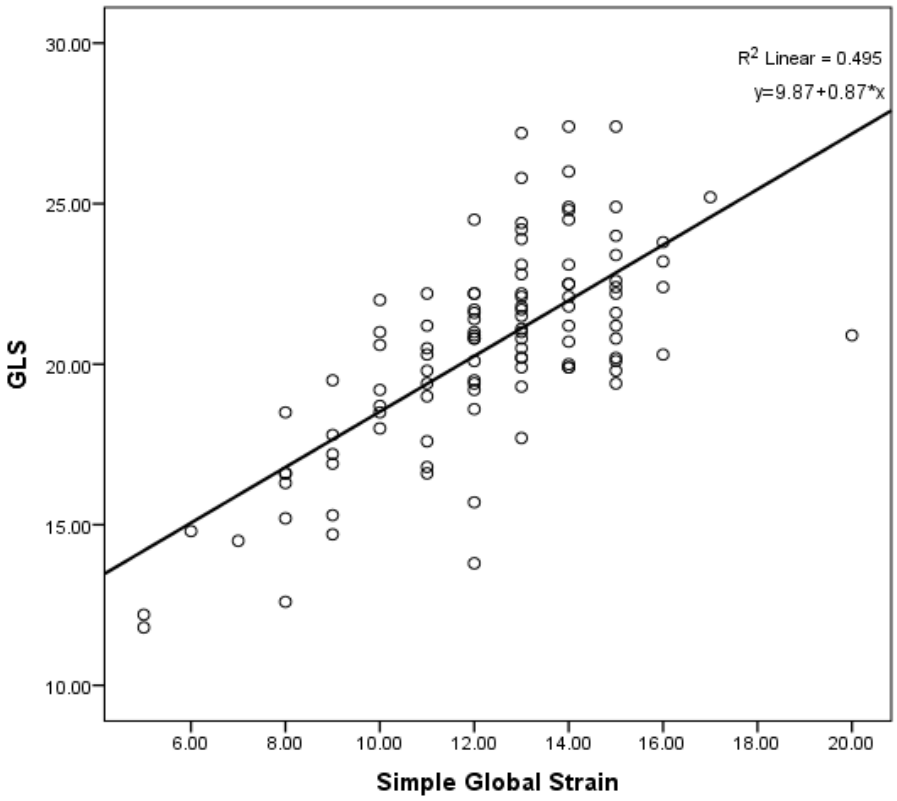

Fig.15 *Linear regression between the global simple method and GLS using the simple global method as an independent factor. The correlation coefficient was 0.87 (confidence interval: 0.7-1.0) P-value < 0.001. The unstandardized equation was* $\tilde{Y}=9.87+0.87(x)$

Variability of measurements

The inter-observer variability was assessed in 22 randomly selected patients for the simplified method and GLS. The results are in Table 4. In Bland-Altman analysis there were a small bias (0.11) and narrow limits of agreement (1.96 x SD): -0.5 to 0.73. Compared to simple strain the inter-observer variability of GLS measurements was worse the mean absolute difference was about 3 times higher (table 5). The corresponding measurements using the GLS method were worse: The mean absolute difference was 1.0±0.7%, the mean relative standard error was 5.4% and the coefficient of variation was 3.8%. Table 5 shows the inter-observer variability for the simple strain measurements obtained globally and from the individual apical views and LV walls. In Bland-Altman analysis of the global simple strain values there were a small bias (-0.18%) and narrow limits of agreement (-1.2 to 0.85%).

Table 4 *Inter-observer variability of simple strain measurements in individual walls, the 2-chamber and 4-chamber views and the average of the 2-chamber and 4-chamber views. The same measurements were performed to test the beat to beat variability.*

Strain	Mean absolute difference	Coefficient of Variation	Relative mean error
Septal wall	0.47 ± 0.37%	3.7%	5.2%
Lateral wall	0.61 ± 0.63%	4.1%	5.8%
Anterior wall	0.37 ± 0.41%	3.4%	4.9%
Inferior wall	0.45 ± 0.51%	3.2%	4.5%
4-Chamber view	0.43 ± 0.4%	3.0%	4.3%
2-Chamber view	0.37 ± 0.33%	2.6%	3.6%
Global (average of 2-chamber view and 4-chamber view)	0.25 ± 0.22%	1.7%	2.4%

The beat to beat variability of GLS and global simple strain was assessed in 12 patients in the simplified method and GLS. For the simple strain method the mean absolute difference was 0.43±0.32%, the mean relative standard error was 3.7% and the coefficient of variation 2.6%. The corresponding values were higher when GLS measurements of different beats were compared (see table 5)

Table 5 *Interobserver variability in simple longitudinal strain measured in 20 patients*

View	Absolute mean difference ± SD	Coefficient of Variation	Relative mean error
2-chamber longitudinal strain	1.5 ± 1.3%	5.7%	8.2%
3-chamber longitudinal strain	2.1 ± 2.0%	7.8%	11.0%
4-chamber longitudinal strain	1.6 ± 2.2%	6.5%	9.1%
Average of the three apical views (GLS)	1.0 ± 1.1%	3.9%	5.6%
Beat to beat variability in GLS	1.0 ± 0.7%	3.8%	5.4%

Discussion:

To our knowledge this is the first study to demonstrate the feasibility and reproducibility of the simple strain method in patients assessed for chemotherapy induced cardiotoxicity. Recently the results of a similar study have been published by a research team in Heidelberg (Aurich et al.).[49] They compared GLS and simple strain in patients with dilated cardiomyopathy and matched healthy controls.[49] They concluded that both the diagnostic and prognostic performance were similar. The simple strain method appears to be a reasonable method for those patients in whom no reliable tracking of GLS can be obtained because of poor image quality. Our results are in line with those from Aurich et al, in terms of good correlation with GLS.

GLS has been used widely for monitoring cardiac toxicities in oncology patients.[35] However, there is a major variability of measurements because the tracking of the entire myocardium is necessary throughout the cardiac cycle. No all LV segments can be readily visualized and errors in tracking are frequent. The simplified method only depends on tracking of few small areas such as the mitral ring and the apical pericardium. Because of the high content of fibrous tissue, the ultrasound signals from these areas are usually less affected by noise than the weak signals from myocardial tissue. In particular the tracking of the mitral annulus can be performed in most patients with otherwise poor acoustic windows.[24,50]

Because of the variability of conventional strain measurements, it is not surprising that the correlation plots between simple strain and GLS show a wide scatter around the regression line and the regression line is not intersecting 0. In this study, only those patients were included in whom tracking for GLS measurement appeared to be feasible. However, that did not mean, that there was optimal tracking of the entire myocardium. In particular the apical myocardium can be difficult to track. Many echocardiographers have to perform strain measurements on suboptimal recordings. Therefore, the current echocardiographic GLS method is not an ideal gold standard for the proposed simple stain method and a correlation with cardiac MRI may need to be confirmed in the future studies.

Simple strain measurements are less variable than GLS measurements.

Among strain measurements tracking the myocardium, GLS has the highest reproducibility.[51] Segmental longitudinal strain is however, poorly reproducible, and therefore GLS as a single value averaging the longitudinal strain obtained in the 2-chamber, 3-chamber and 4-chamber views is the only value recommended to detect early myocardial damage from cancer drugs.[47,52] In a study performed by Sawaya et al., the change in longitudinal strain in 4-chamber and 2-chamber views was found to be a predictive of development of heart failure in 81 patients, but not radial or circumferential strain. In another study the change in GLS (this time from the 3 apical views) showed similar results and was superior to other echocardiographic parameters like S' and e'.

In a recent study planned by EACVI/ASE/industry 'Task Force to Standardize Deformation Imaging' among different vendors inter- and intra-observer variability was tested for GLS and compared to other conventional echocardiographic parameters in 63 healthy volunteers.[48] The absolute GLS values ranged between 18% and 21.5%. The absolute difference between vendors was 3.7% and was statistically significant (P<0.001). The inter-observer relative mean error ranged from 5.4% to 8.6%. In Philips echocardiography machines the mean absolute GLS was 18.8 ± 3.6% and the inter-observer relative mean error was 6.2% (Fig.16). In our study the mean GLS was similar (20.5 ± 2.6%). The inter-observer relative mean error was slightly better, 5.6%. Our new simplified method had a statistically significantly lower inter-observer relative mean error of 2.4% (p=0.04).

Because of the low variability of simple strain measurements, it appears to be reasonable to use only the measurements in 4- and 2-chamber view for global simple strain. These two views are used for measurement of the LV ejection fraction as a measure of global systolic function. This means a further simplification compared to the GLS method. The measurements in a subgroup of our patients showed that the simple strain values from 2 apical views are not different from the values obtained from all 3 views. In patients with regional wall motion abnormalities, however, it is reasonable to assess all 3 apical views.

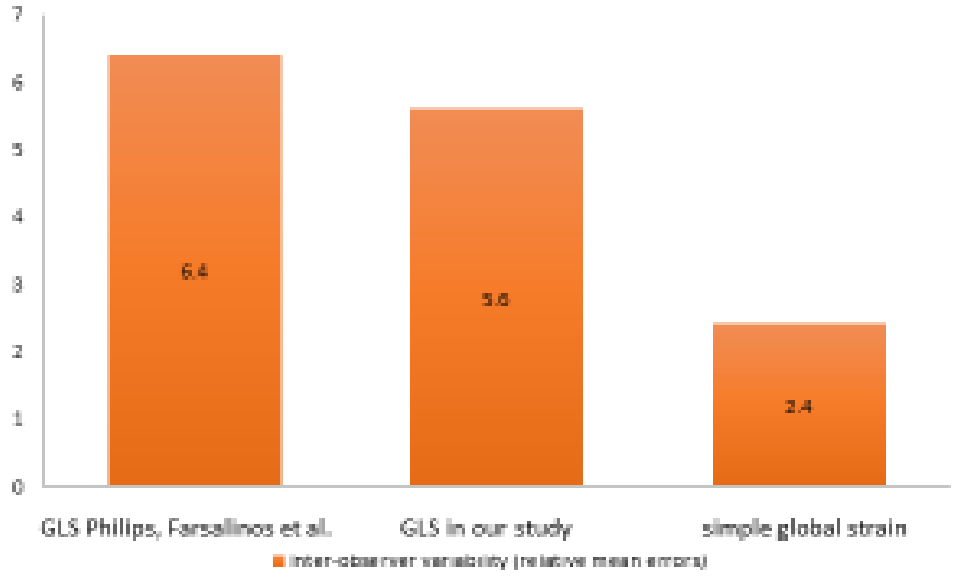

Fig.16 *The relative mean errors in GLS for Philips echocardiography machines according to Farsalinos, Voigt et al.[48] GLS in our study and global strain using the new simplified method. The "*" indicates statistical significance (p < 0.05).*

The values for our new simplified method as expected, are significantly lower than the GLS values. This was reported by Aurich et al.[49] In their study, the normal value for healthy controls was 16.3 ± 1.5%. The difference was due to the geometrical difference in length shortening between the two methods. The % change of the curved myocardium is higher than the change in length of the line connecting the mitral ring and the LV apex (Fig.17).

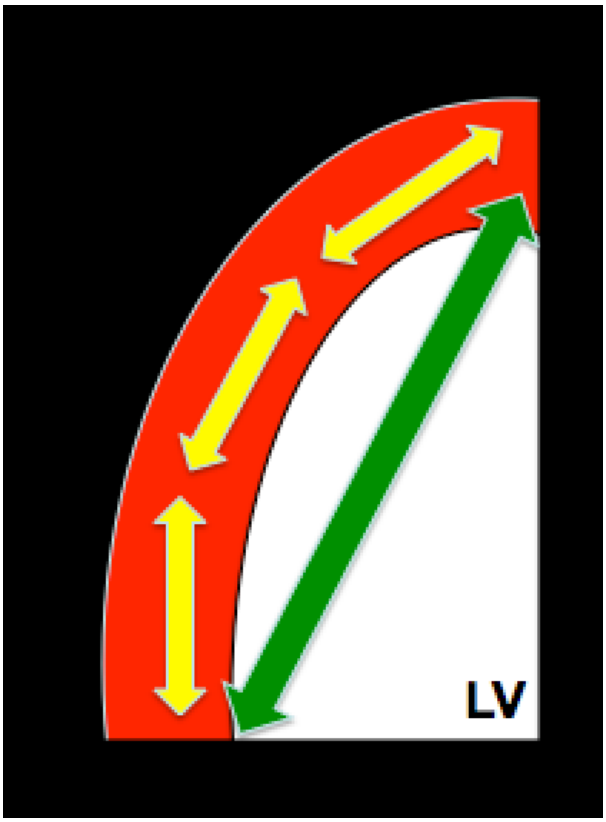

Fig.17 *Shortening of the myocardium assessed by GLS (yellow arrows) vs simple strain (green arrow)*

Simple strain is a method for assessment of the global LV function. It relies on tracking of fibrous tissue rather than on tracking of the myocardium. Therefore, this technique does not allow for analysis of segmental LV function. But in principle in all clinical scenarios where currently GLS is applied, simple strain measurements may be considered such as in patients undergoing chemotherapy or in ICU patients with often suboptimal image quality. These patients usually are assessed with contrast echocardiography for assessment of the LV ejection fraction.[53] However, GLS measurements do not improve when ultrasound contrast agents are injected due to interference of the contrast microbubbles with the speckle tracking tools of most manufacturers.[46]

Limitations:

This was not an optimal study to obtain normal values of simple strain. The echocardiograms analyzed in this study were obtained from patients with breast cancer undergoing chemotherapy with cardiotoxic drugs. However, the majority of them had GLS values of >20% which is regarded as normal as well as normal EF.[9,20] In this patient group, measurements of simple strain were lower than those for GLS. This is very similar to the data of the Heidelberg group.[49] In order to establish benchmark for simple strain further studies in larger groups of healthy individuals are needed.

The measurement of simple strain was performed using the Q-lab post processing tool which was provided by Philips for speckle tracking analysis and is currently not available from other manufacturers. In principle every system which is capable of GLS can also be modified to provide simple strain measurements. Further studies showing the robustness of simple strain probably will motivate other manufacturers to include simple strain in their analysis tools.

Although simple strain overcomes the limitations of poor acoustic windows, it still depends on adequate 4- and 2-chamber views and will be inaccurate in foreshortened imaging planes. This is no different from GLS measurements. In principle the simple strain method can be applied on reconstructed 4- and 2-chamber vies of 3D datasets in order to minimize the risk of analyzing foreshortened imaging planes.

The simple strain method appears to be particularly suitable for patients in whom standard tracking for GLS assessment does not work. This could not be demonstrated in this study. This study was designed as a pilot study to explore whether the variability of the simple strain method and whether there is a correlation of the simple strain measurements with GLS values. Further studies are needed to demonstrate the clinical utility of simple strain in patients with poor

acoustic windows. For these studies cardiac MRI appears to be the reference method to compare with.

Future:

This is a proof of concept study. It shows good correlation with GLS in oncology patients. The next step would be to establish normal values. This will require a study with a larger population and with different subgroups of patients. Also, this method could be developed and used in a 3D data set, which could solve another significant limitation which is foreshortening. We also see a potential of assessing the strain rate using the simple strain method.

Conclusion:

Simple strain is a promising method to assess longitudinal function. The tracking of few structures with stable echogenicity reduces the variability of measurements compared to conventional strain measurements which depend on tracking of the entire myocardium and are frequently confounded by noise. There is a strong linear correlation of simple strain and GLS. Further clinical studies are warranted to establish normal values and further explore the clinical utility for assessment of global longitudinal LV function.

References

1. Solomon SD, Skali H, Anavekar NS, et al. Changes in ventricular size and function in patients treated with valsartan, captopril, or both after myocardial infarction. Circulation 2005;111(25):3411–9.

2. St John Sutton M, Pfeffer MA, Moye L, et al. Cardiovascular death and left ventricular remodeling two years after myocardial infarction: baseline predictors and impact of long-term use of captopril: information from the Survival and Ventricular Enlargement (SAVE) trial. Circulation 1997;96(10):3294–9.

3. DeCara JM, Toledo E, Salgo IS, Lammertin G, Weinert L, Lang RM. Evaluation of Left Ventricular Systolic Function Using Automated Angle-Independent Motion Tracking of Mitral Annular Displacement. Journal of the American Society of Echocardiography 2005;18(12):1266–9.

4. Spencer KT, Bednarz J, Mor-Avi V, DeCara J, Lang RM. Automated endocardial border detection and evaluation of left ventricular function from contrast-enhanced images using modified acoustic quantification. Journal of the American Society of Echocardiography 2002;15(8):777–81.

5. Mondillo S, Galderisi M, Mele D, et al. Speckle-tracking echocardiography: a new technique for assessing myocardial function. J Ultrasound Med 2011;30(1):71–83.

6. Shah AM, Solomon SD. Myocardial deformation imaging: current status and future directions. Circulation 2012;125(2):e244–8.

7. Lima JA, Jeremy R, Guier W, et al. Accurate systolic wall thickening by nuclear magnetic resonance imaging with tissue tagging: correlation with sonomicrometers in normal and ischemic myocardium. JAC 1993;21(7):1741–51.

8. Buchalter MB, Weiss JL, Rogers WJ, et al. Noninvasive quantification of left ventricular rotational deformation in normal humans using magnetic resonance imaging myocardial tagging. Circulation 1990;81(4):1236–44.

9. Voigt JU, Pedrizzetti G, Lysyansky P, et al. Definitions for a common standard for 2D speckle tracking echocardiography: consensus document of the EACVI/ASE/Industry Task Force to standardize deformation imaging. Eur Heart J Cardiovasc Imaging 2015;16(1):1–11.

10. Langeland S. Experimental Validation of a New Ultrasound Method for the Simultaneous Assessment of Radial and Longitudinal Myocardial Deformation Independent of Insonation Angle. Circulation 2005;112(14):2157–62.

11. Bohs LN, Friemel BH, McDermott BA, Trahey GE. A real time system for quantifying and displaying two-dimensional velocities using ultrasound.

Ultrasound Med Biol 1993;19(9):751–61.

12. Insana MF, Wagner RF, Garra BS, Momenan R, Shawker TH. Pattern recognition methods for optimizing multivariate tissue signatures in diagnostic ultrasound. Ultrason Imaging 1986;8(3):165–80.

13. Xiao H, Bruhns OT, Meyers A. Basic Issues Concerning Finite Strain Measures and Isotropic Stress-Deformation Relations. Journal of Elasticity 2002;67(1):1–23.

14. Voigt J-U, Pedrizzetti G, Lysyansky P, et al. Definitions for a Common Standard for 2D Speckle Tracking Echocardiography: Consensus Document of the EACVI/ASE/Industry Task Force to Standardize Deformation Imaging. Journal of the American Society of Echocardiography 2015;28(2):183–93.

15. Sengupta PP, Korinek J, Belohlavek M, et al. Left Ventricular Structure and Function. Journal of the American College of Cardiology 2006;48(10):1988–2001.

16. Greenbaum RA, Ho SY, Gibson DG, Becker AE, Anderson RH. Left ventricular fibre architecture in man. Br Heart J 1981;45(3):248–63.

17. Voigt J-U, Lindenmeier G, Exner B, et al. Incidence and characteristics of segmental postsystolic longitudinal shortening in normal, acutely ischemic, and scarred myocardium. Journal of the American Society of Echocardiography 2003;16(5):415–23.

18. MD ROM, PhD PL, MD AMD, MSc JD, PhD J-UVM. How to Define End-Diastole and End-Systole? JACC Cardiovasc Imaging 2015;8(2):148–57.

19. Mor-Avi V, Lang RM, Badano LP, et al. Current and evolving echocardiographic techniques for the quantitative evaluation of cardiac mechanics: ASE/EAE consensus statement on methodology and indications endorsed by the Japanese Society of Echocardiography. Eur J Echocardiogr 2011;12(3):167–205.

20. Lang RM, Badano LP, Mor-Avi V, et al. Recommendations for cardiac chamber quantification by echocardiography in adults: an update from the American Society of Echocardiography and the European Association of Cardiovascular Imaging. Eur Heart J Cardiovasc Imaging 2015;16(3):233–70.

21. Takeuchi M, Otsuji Y, Lang RM. Evaluation of left ventricular function using left ventricular twist and torsion parameters. Curr Cardiol Rep 2009;11(3):225–30.

22. Takeuchi M, Nishikage T, Nakai H, Kokumai M, Otani S, Lang RM. The assessment of left ventricular twist in anterior wall myocardial infarction using two-dimensional speckle tracking imaging. J Am Soc Echocardiogr 2007;20(1):36–44.

23. de Knegt MC, Biering-Sorensen T, Sogaard P, Sivertsen J, Jensen JS, Mogelvang R.

Concordance and reproducibility between M-mode, tissue Doppler imaging, and two-dimensional strain imaging in the assessment of mitral annular displacement and velocity in patients with various heart conditions. Eur Heart J Cardiovasc Imaging 2013;15(1):62–9.

24. MD WT, MD HA, MD ARP, et al. Rapid Estimation of Left Ventricular Function Using Echocardiographic Speckle-Tracking of Mitral Annular Displacement. Journal of the American Society of Echocardiography 2010;23(5):511–5.

25. Kukulski T, Jamal F, Herbots L, et al. Identification of acutely ischemic myocardium using ultrasonic strain measurements. A clinical study in patients undergoing coronary angioplasty. JAC 2003;41(5):810–9.

26. Takayama M, Norris RM, Brown MA, Armiger LC, Rivers JT, White HD. Postsystolic shortening of acutely ischemic canine myocardium predicts early and late recovery of function after coronary artery reperfusion. Circulation 1988;78(4):994–1007.

27. Mirea O, Duchenne J, Voigt J-U. Recent advances in echocardiography: strain and strain rate imaging. F1000Res 2016;5.

28. Kalam K, Otahal P, Marwick TH. Prognostic implications of global LV dysfunction: a systematic review and meta-analysis of global longitudinal strain and ejection fraction. Heart 2014;100(21):1673–80.

29. Authors/Task Force members, Elliott PM, Anastasakis A, et al. 2014 ESC Guidelines on diagnosis and management of hypertrophic cardiomyopathy: the Task Force for the Diagnosis and Management of Hypertrophic Cardiomyopathy of the European Society of Cardiology (ESC). Eur. Heart J. 2014;35(39):2733–79.

30. Liu D, Hu K, Nordbeck P, Ertl G, Störk S, Weidemann F. Longitudinal strain bull's eye plot patterns in patients with cardiomyopathy and concentric left ventricular hypertrophy. Eur J Med Res 2016;21(1):21.

31. Phelan D, Collier P, Thavendiranathan P, et al. Relative apical sparing of longitudinal strain using two-dimensional speckle-tracking echocardiography is both sensitive and specific for the diagnosis of cardiac amyloidosis. Heart 2012;98(19):1442–8.

32. Krämer J, Niemann M, Liu D, et al. Two-dimensional speckle tracking as a non-invasive tool for identification of myocardial fibrosis in Fabry disease. Eur Heart J 2013;34(21):1587–96.

33. Nishimura RA, Otto CM, Bonow RO, et al. 2014 AHA/ACC Guideline for the Management of Patients With Valvular Heart Disease: executive summary: a report of the American College of Cardiology/American Heart Association Task

Force on Practice Guidelines. American Heart Association, Inc; 2014. p. 2440–92.

34. Donal E, Thebault C, O'Connor K, et al. Impact of aortic stenosis on longitudinal myocardial deformation during exercise. Eur J Echocardiogr 2011;12(3):235–41.

35. Thavendiranathan P, Poulin F, Lim K-D, Plana JC, Woo A, Marwick TH. Use of myocardial strain imaging by echocardiography for the early detection of cardiotoxicity in patients during and after cancer chemotherapy: a systematic review. Journal of the American College of Cardiology 2014;63(25 Pt A):2751–68.

36. King A, Thambyrajah J, Leng E, Stewart MJ. Global longitudinal strain: a useful everyday measurement? Echo Research and Practice 2016;3(3):85–93.

37. Sawaya H, Sebag IA, Plana JC, et al. Assessment of echocardiography and biomarkers for the extended prediction of cardiotoxicity in patients treated with anthracyclines, taxanes, and trastuzumab. Circ Cardiovasc Imaging 2012;5(5):596–603.

38. Pituskin E, Mackey JR, Koshman S, et al. Multidisciplinary Approach to Novel Therapies in Cardio-Oncology Research (MANTICORE 101-Breast): A Randomized Trial for the Prevention of Trastuzumab-Associated Cardiotoxicity. J Clin Oncol 2017;35(8):870–7.

39. Tang ASL, Wells GA, Talajic M, et al. Cardiac-resynchronization therapy for mild-to-moderate heart failure. N Engl J Med 2010;363(25):2385–95.

40. Seo Y, Ishizu T, Machino T et al. Incremental Value of Speckle Tracking Echocardiography to Predict Cardiac Resynchronization Therapy (CRT) Responders. JAMA 2016; 5(16):

41. Shanks M, Antoni ML, Hoke U, et al. The effect of cardiac resynchronization therapy on left ventricular diastolic function assessed with speckle-tracking echocardiography. Eur J Heart Fail 2011;13(10):1133–9.

42. Shanks M, Ng ACT, van de Veire NRL, et al. Incremental prognostic value of novel left ventricular diastolic indexes for prediction of clinical outcome in patients with ST-elevation myocardial infarction. Am J Cardiol 2010;105(5):592–7.

43. Trahey GE, Hubbard SM, Ramm von OT. Angle independent ultrasonic blood flow detection by frame-to-frame correlation of B-mode images. Ultrasonics 1988;26(5):271–6.

44. Wagner RF, Insana MF, Smith SW. Fundamental correlation lengths of coherent speckle in medical ultrasonic images. IEEE Trans Ultrason Ferroelectr Freq Control 1988;35(1):34–44.

45. Cho GY, Marwick TH, Kim HS, Kim MK, Hong KS, Oh DJ. Global 2-Dimensional Strain as a New Prognosticator in Patients With Heart Failure. JAC 2009;54(7):618–24.

46. Huqi A, He A, Klas B, et al. Myocardial deformation analysis in contrast echocardiography: first results using two-dimensional cardiac performance analysis. J Am Soc Echocardiogr 2013;26(11):1282–9.

47. FESC RMLMF, FESC LPBMP, FASE VM-AP, et al. Recommendations for Cardiac Chamber Quantification by Echocardiography in Adults: An Update from the American Society of Echocardiography and the European Association of Cardiovascular Imaging. Journal of the American Society of Echocardiography 2015;28(1):1–39.e14.

48. Farsalinos KE, Daraban AM, Ünlü S, Thomas JD, Badano LP, Voigt J-U. Head-to-Head Comparison of Global Longitudinal Strain Measurements among Nine Different Vendors: The EACVI/ASE Inter-Vendor Comparison Study. J Am Soc Echocardiogr 2015;28(10):1171–1181–e2.

49. Aurich M, Fuchs P, Müller-Hennessen M, et al. Unidimensional Longitudinal Strain: A Simple Approach for the Assessment of Longitudinal Myocardial Deformation by Echocardiography. J Am Soc Echocardiogr 2018;31(6):733–42.

50. Frielingsdorf J, Schmidt C, Debrunner M, et al. Atrium-driven mitral annulus motion velocity reflects global left ventricular function and pulmonary congestion during acute biventricular pacing. J Am Soc Echocardiogr 2008;21(3):288–93.

51. Risum N, Ali S, Olsen NT, et al. Variability of global left ventricular deformation analysis using vendor dependent and independent two-dimensional speckle-tracking software in adults. J Am Soc Echocardiogr 2012;25(11):1195–203.

52. Chair JCPMF, Co-Chair MGMF, PhD ABM, et al. Expert Consensus for Multimodality Imaging Evaluation of Adult Patients during and after Cancer Therapy: A Report from the American Society of Echocardiography and the European Association of Cardiovascular Imaging. Journal of the American Society of Echocardiography 9999;27(9):911–39.

53. Zamorano JL, Lancellotti P, Rodriguez Muñoz D, et al. 2016 ESC Position Paper on cancer treatments and cardiovascular toxicity developed under the auspices of the ESC Committee for Practice Guidelines: The Task Force for cancer treatments and cardiovascular toxicity of the European Society of Cardiology (ESC). Eur. Heart J. 2016;37(36):2768–801.

Appendix

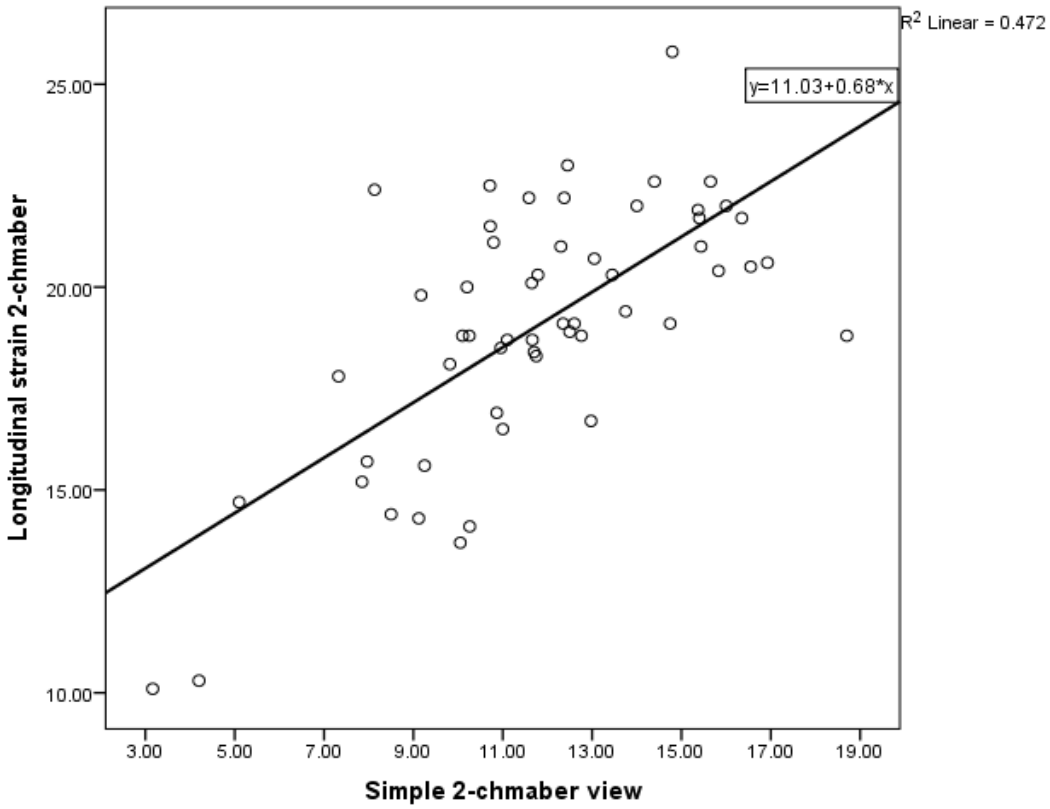

Fig.I Linear regression between the simple strain measured in the 2-chamber view and the longitudinal strain obtained from the 2-chamber view using the simple 2-chamber as an independent factor ($P < 0.001$), correlation coefficient 0.68.

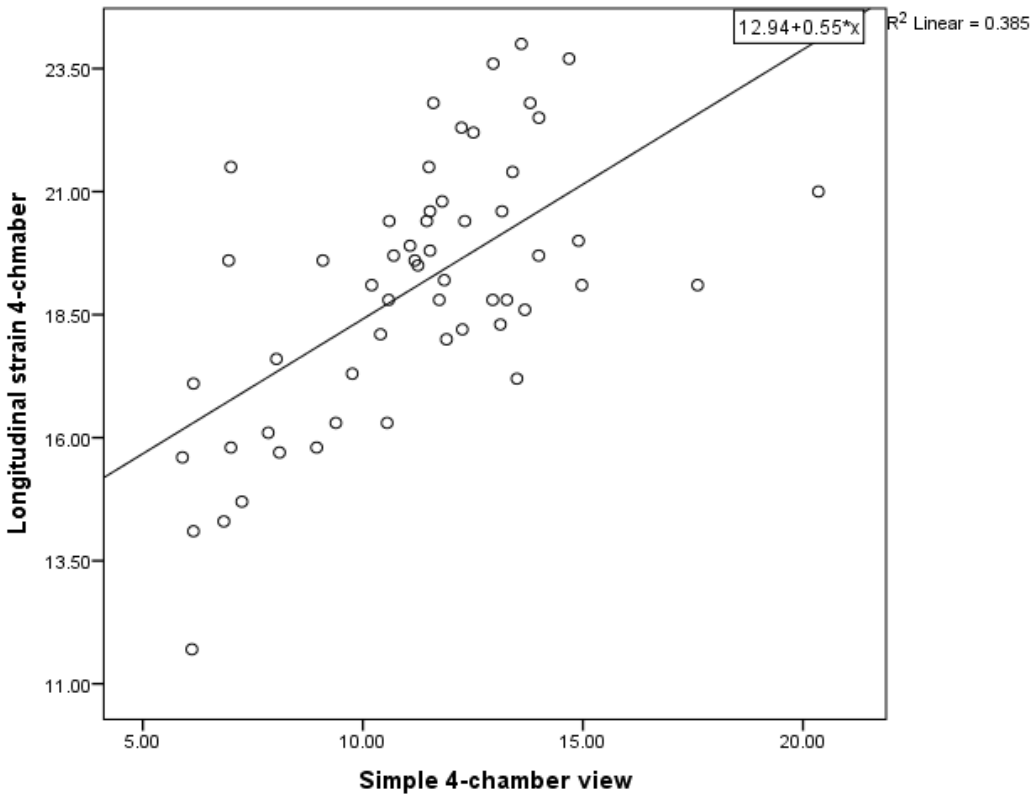

Fig.II Linear regression between the simple strain measured in the 4-chamber view and the longitudinal strain obtained from the 4-chamber view using the simple 2-chamber as an independent factor ($P < 0.001$), correlation coefficient 0.55.

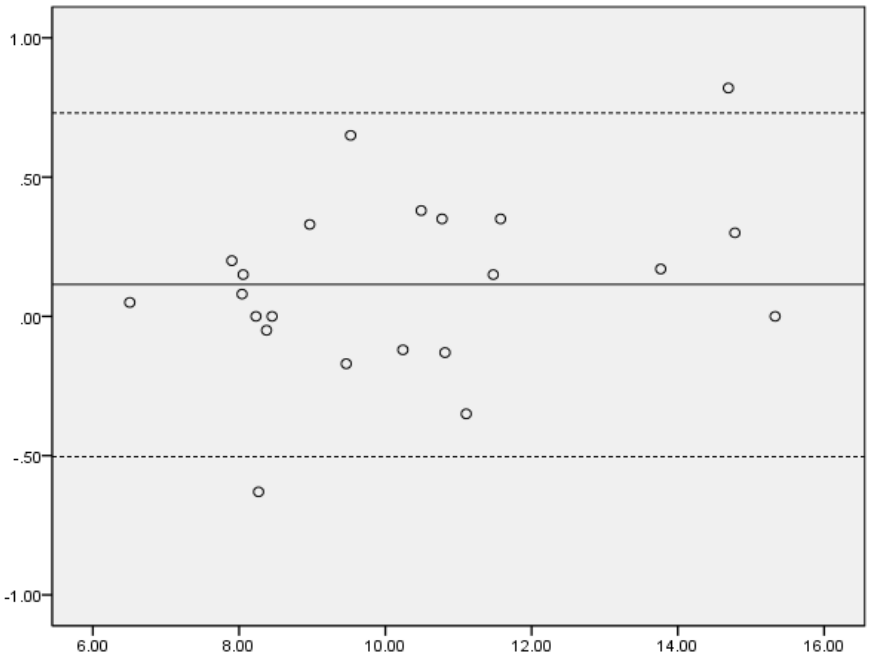

Fig. III Bland-Altman plot showing individual values of the global simple method of both investigators and the mean (y-axis) vs the mean of the investigators (x-axis) The solid line indicates the bias (0.11%) and interrupted lines the limit of agreement (-0.5 to 0.73%).

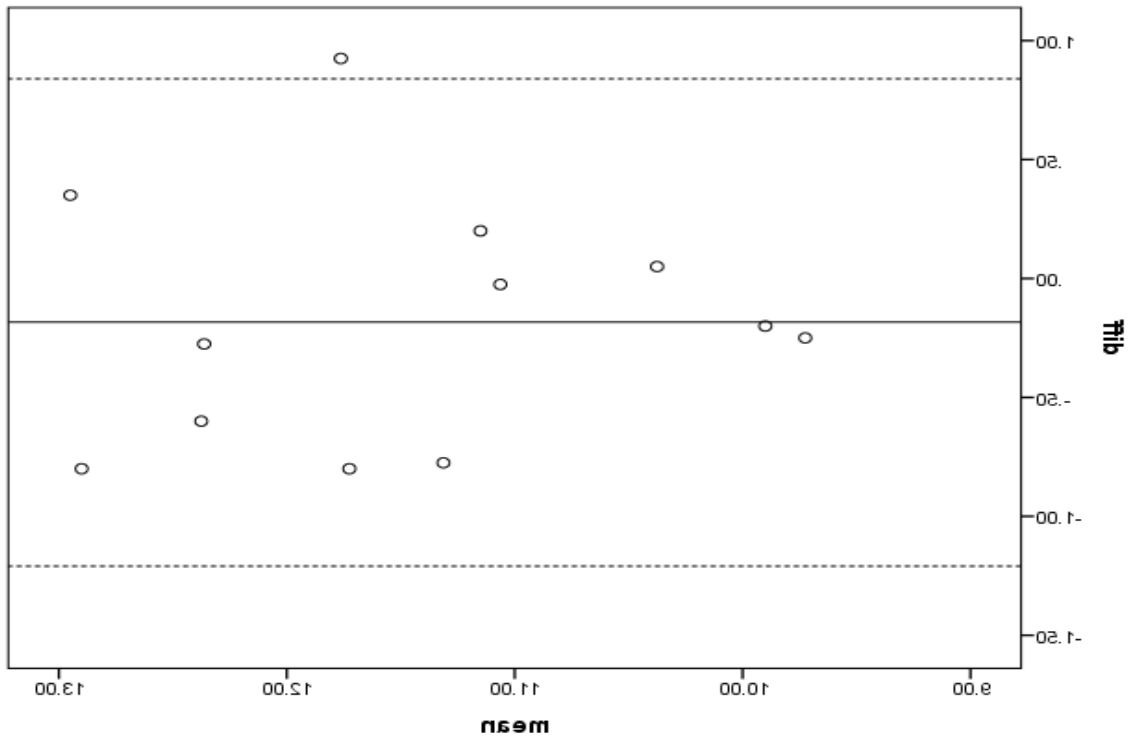

Fig.IV Bland-Altman plot showing the agreement in beat to beat variability. The mean (y-axis) vs the mean of the different beat (x-axis) The solid line indicate the bias (-0.18%) and interrupted lines the limit of agreement (-1.2 to 0.85%).